

# **Hydrogen Separation Membranes Annual Report for FY 2007**

---

**Energy Systems Division**

**About Argonne National Laboratory**

Argonne is a U.S. Department of Energy laboratory managed by UChicago Argonne, LLC under contract DE-AC02-06CH11357. The Laboratory's main facility is outside Chicago, at 9700 South Cass Avenue, Argonne, Illinois 60439. For information about Argonne, see [www.anl.gov](http://www.anl.gov).

**Availability of This Report**

This report is available, at no cost, at <http://www.osti.gov/bridge>. It is also available on paper to the U.S. Department of Energy and its contractors, for a processing fee, from:

U.S. Department of Energy  
Office of Scientific and Technical Information  
P.O. Box 62  
Oak Ridge, TN 37831-0062  
phone (865) 576-8401  
fax (865) 576-5728  
[reports@adonis.osti.gov](mailto:reports@adonis.osti.gov)

**Disclaimer**

This report was prepared as an account of work sponsored by an agency of the United States Government. Neither the United States Government nor any agency thereof, nor UChicago Argonne, LLC, nor any of their employees or officers, makes any warranty, express or implied, or assumes any legal liability or responsibility for the accuracy, completeness, or usefulness of any information, apparatus, product, or process disclosed, or represents that its use would not infringe privately owned rights. Reference herein to any specific commercial product, process, or service by trade name, trademark, manufacturer, or otherwise, does not necessarily constitute or imply its endorsement, recommendation, or favoring by the United States Government or any agency thereof. The views and opinions of document authors expressed herein do not necessarily state or reflect those of the United States Government or any agency thereof, Argonne National Laboratory, or UChicago Argonne, LLC.

# Hydrogen Separation Membranes Annual Report for FY 2007

---

by

U. (Balu) Balachandran

Energy Systems Division, Argonne National Laboratory

contributors

L. Chen, S.E. Dorris, J.E. Emerson, T.H. Lee,

C.Y. Park, J.J. Picciolo, and S.J. Song

work supported by

U.S. Department of Energy

Office of Fossil Energy, National Energy Technology Laboratory

January 31, 2008

## Contents

---

I.	Objective .....	1
II.	Highlights .....	1
III.	Introduction .....	2
IV.	Results .....	3
	Milestone 1. Determine stability of membrane in steam-containing atmosphere. ....	3
	Milestone 2. Determine the Pd/Pd <sub>4</sub> S phase boundary at low H <sub>2</sub> concentrations.....	9
	Milestone 3. Test membrane in high-pressure feed streams with higher H <sub>2</sub> concentration.. ....	13
	Milestone 4. Fabricate and evaluate tubular membrane.....	16
V.	Future Work.....	23
VI.	Publications and Presentations .....	24
	References .....	30

## Figures

---

1. Water vapor pressure-dependence of H <sub>2</sub> flux at 600 and 900°C for ANL-3e membrane (≈0.22 mm thick).....	4
2. Time-dependence of H <sub>2</sub> flux for 0.15-mm-thick ANL-3e membrane using 50% H <sub>2</sub> /2% H <sub>2</sub> O/balance He as feed gas. ....	5
3. Time-dependence of hydrogen flux for 0.27-mm-thick ANL-3e membrane at 600-900°C using dry and humidified syngas as feed. ....	6
4. Calculated gas composition for: a) dry gas containing 52.7% H <sub>2</sub> /10.1% CO/8.0% CO <sub>2</sub> /0.6% CH <sub>4</sub> /balance He and b) humidified gas containing 52.7% H <sub>2</sub> /20.6% H <sub>2</sub> O/10.1% CO/8.0% CO <sub>2</sub> /0.6% CH <sub>4</sub> /balance He.....	7
5. Hydrogen flux through 0.27-mm-thick ANL-3e membrane using 50% CO/balance H <sub>2</sub> O as feed gas. ....	8
6. Total hydrogen production rate of 0.27-mm-thick ANL-3e membrane using 50% CO/balance H <sub>2</sub> O as feed gas. ....	8
7. Pd/Pd <sub>4</sub> S phase boundary for gases containing 73% and 10% H <sub>2</sub> , calculated using data from literature and determined at Argonne.....	10
8. Equilibrium constant for formation of Pd <sub>4</sub> S .....	11
9. Pd/Pd <sub>4</sub> S phase boundary for gases containing 73% and 10% H <sub>2</sub> , calculated using fit of Argonne's experimental data.....	12
10. Hydrogen flux vs. $\Delta p\text{H}_2^{1/2}$ for ANL-3 membranes tested in high-pressure reactors at Argonne and NETL .....	14
11. Hydrogen flux of ANL-3 membranes measured by varying pH <sub>2</sub> in high-pressure reactors at Argonne and NETL and by varying mol.% H <sub>2</sub> in Argonne's ambient-pressure reactor.....	15
12. Porous alumina tube after pre-sintering and two porous alumina tubes and ANL-3e film on porous alumina tube after sintering .....	16
13. Porous alumina tube coated with dense ANL-3e film on spring-loaded fixture used to measure tube's hydrogen flux.....	17
14. Hydrogen flux for tubular ANL-3 thin film on porous Al <sub>2</sub> O <sub>3</sub> . Thin film contained Pd (60 vol.%)/CeO <sub>2</sub> and had thickness of ≈30 μm.....	18
15. Hydrogen permeability for tubular ANL-3 thin film on porous Al <sub>2</sub> O <sub>3</sub> . Thin film contained Pd (60 vol.%)/CeO <sub>2</sub> and had thickness of ≈30 μm. ....	18

16. Cross-sectional views of 58- $\mu\text{m}$ -thick Pd(60 vol.%)/TZ-3Y film on porous $\text{Al}_2\text{O}_3$ tube. ....	19
17. Hydrogen flux for 58- $\mu\text{m}$ -thick Pd(60 vol.%)/TZ-3Y film on porous $\text{Al}_2\text{O}_3$ measured with feed flowing inside tube and sweep outside tube, or feed outside tube and sweep inside. ....	20
18. Hydrogen permeability for 58- $\mu\text{m}$ -thick Pd(60 vol.%)/TZ-3Y film on porous $\text{Al}_2\text{O}_3$ measured with feed flowing inside tube and sweep outside tube, or feed outside tube and sweep inside. ....	20
19. $\text{H}_2$ flux for 58- $\mu\text{m}$ -thick Pd(60 vol.%)/TZ-3Y film on porous $\text{Al}_2\text{O}_3$ tube measured with various gas flow rates (ml/min) .....	21
20. $\text{H}_2$ permeability for 58- $\mu\text{m}$ -thick Pd(60 vol.%)/TZ-3Y film on porous $\text{Al}_2\text{O}_3$ tube measured with various gas flow rates (ml/min) .....	22

## Tables

---

1. Free energy of formation for $\text{Pd}_4\text{S}$ calculated from Argonne's data and data in literature .....	13
---	----

**HYDROGEN SEPARATION MEMBRANES -- ANNUAL REPORT FOR FY 2007**  
**ARGONNE NATIONAL LABORATORY**

Project Title: Development of Dense Ceramic Membranes for Hydrogen Separation

NETL Project Manager: Richard Dunst

ANL Project PI: U. (Balu) Balachandran

B&R Code/Contract Number: AA-10-40-00-0 & AA-20-15-00-0/FWP 49601

Report Date: January 31, 2008

**I. OBJECTIVE**

The objective of this work is to develop dense ceramic membranes for separating hydrogen from other gaseous components in a nongalvanic mode, i.e., without using an external power supply or electrical circuitry.

**II. HIGHLIGHTS**

1. Hydrogen flux measurements showed that ANL-3e membranes are stable:
  - (i) during short-term ( $\approx 1$  h) exposures to feed gas at 600 and 900°C with partial pressure of steam ( $p_{H_2O}$ ) in the range 0.03-0.49 atm;
  - (ii) for  $>150$  h in tests with feed gas composed of 50%  $H_2$ /2%  $H_2O$ /balance He at 500-800°C; and
  - (iii) during short ( $\approx 100$  h) exposures at 600-700°C in feed gas that contained 52.7%  $H_2$ /20.6%  $H_2O$ /10.1% CO/8.0%  $CO_2$ /0.6%  $CH_4$ /balance He.
2. The location of the Pd/Pd<sub>4</sub>S phase boundary was determined in tests using feed gas that contained 10%  $H_2$  and 8-50 ppm  $H_2S$ .
3. The hydrogen flux was measured through a disk-shaped ANL-3e sample in tests using Argonne's high-pressure reactor with feed gas of 90%  $H_2$ /balance He at temperatures up to 900°C and pressures up to 300 psig.
4. Methods for fabricating tubular hydrogen separation membranes were developed during FY 2007. The tubes contain a dense film of an ANL-3 type membrane on a porous alumina support.
5. Permeability values for a tube made with Pd (60 vol.%)/ $Y_2O_3$ -stabilized  $ZrO_2$  were close to the expected values, based on permeability values found in the literature for palladium and the volume fraction of palladium in the membrane.

### III. INTRODUCTION

The goal of this project is to develop dense hydrogen transport membranes (HTMs) that nongalvanically (i.e., without electrodes or external power supply) separate hydrogen from gas mixtures at commercially significant fluxes under industrially relevant operating conditions. HTMs will be used to separate hydrogen from gas mixtures such as the product streams from coal gasification, methane partial oxidation, and water-gas shift reactions. Potential ancillary uses of HTMs include dehydrogenation and olefin production, as well as hydrogen recovery in petroleum refineries and ammonia synthesis plants, the largest current users of deliberately produced hydrogen. This report describes progress that was made during FY 2007 on the development of HTM materials.

Our materials development for the HTM follows a three-pronged approach. In one approach, we utilize principles of solid-state defect chemistry to properly dope selected monolithic electronic/protonic conductors (perovskites doped on both A- and B-sites) to obtain materials that are chemically stable and have suitable protonic and electronic conductivities. The second approach uses cermet (i.e., ceramic/metal composite) membranes that are prepared by homogeneously mixing electronic/protonic conductors with a metallic component. The metal phase in these cermets enhances the hydrogen permeability of the ceramic phase by increasing the electronic conductivity and by providing an additional transport path for the hydrogen if the metal has high hydrogen permeability. In our third approach, we disperse a metal with high hydrogen permeability (called a “hydrogen transport metal”) in a support matrix composed of either a ceramic or a metal. In these composites, hydrogen is transported almost exclusively through the hydrogen transport metal, and the matrix serves primarily as a chemically stable structural support. Our focus during FY 2007 was on the development of HTMs in which a ceramic phase provided structural support for a hydrogen transport metal. In particular, we focused on ANL-3e membranes (composed of Pd mixed with  $\text{Y}_2\text{O}_3$ -stabilized  $\text{ZrO}_2$ ), which have given the highest hydrogen flux to date for membranes made at Argonne ( $\approx 22$  and  $\approx 32$   $\text{cm}^3/\text{min}\cdot\text{cm}^2$  at 500 and 900°C, respectively). Various membranes developed at Argonne are summarized elsewhere. [1]

Good chemical stability is a critical requirement for HTMs due to the corrosive nature of product streams from coal gasification and/or methane reforming. Hydrogen sulfide ( $\text{H}_2\text{S}$ ) is a particularly corrosive contaminant that HTMs are expected to encounter. When  $\text{H}_2\text{S}$  reacts with the ANL-3e membrane, palladium sulfide ( $\text{Pd}_4\text{S}$ ) forms on the surface of the membrane. Because  $\text{Pd}_4\text{S}$  impedes hydrogen permeation through the membrane, the chemical stability of ANL-3e membranes was evaluated by determining the conditions under which  $\text{Pd}_4\text{S}$  forms. The Pd/ $\text{Pd}_4\text{S}$  phase boundary was determined in the temperature range  $\approx 450$ – $650^\circ\text{C}$  in tests using various feed gases that contained 10–73%  $\text{H}_2$  and  $\approx 8$ –400 ppm  $\text{H}_2\text{S}$ . We also began to assess the effect of syngas components on the Pd/ $\text{Pd}_4\text{S}$  phase boundary by locating the phase boundary in feed gas that contained 73%  $\text{H}_2$ /0.497%  $\text{CH}_4$ /6.188%  $\text{CO}_2$ /7.8455%  $\text{CO}$ /400 ppm  $\text{H}_2\text{S}$ /balance He. To assess the effect of steam on hydrogen permeation through ANL-3e membranes, we



tested the chemical stability of an ANL-3e membrane in the presence of steam by measuring its hydrogen flux in feed gas that contained 0.03-0.49 atm H<sub>2</sub>O.

Besides chemical stability in corrosive environments, practical HTMs must have good mechanical integrity at high temperature ( $\approx 900^{\circ}\text{C}$ ) and high pressure ( $\approx 350$  psi). Although the performance of Argonne HTMs has been evaluated in high-pressure tests at the National Energy Technology Laboratory (NETL) [1], a reactor was constructed at Argonne to expand the capability for measuring hydrogen flux at high pressures. Argonne's reactor allows membranes and seals to be tested at temperatures up to  $900^{\circ}\text{C}$  and pressures up to 300 psig. Using this reactor, we measured the hydrogen flux of disk-shaped ANL-3e samples in feed gas that contained either 4% H<sub>2</sub> or 90% H<sub>2</sub> at temperatures up to  $900^{\circ}\text{C}$  and pressures up to  $\approx 300$  psig. Results from these measurements are included in this report. To aid in the development of HTMs that meet the requirements described above, the following milestones were established in the Field Work Proposal for FY 2007:

1. Determine stability of membrane in steam-containing atmosphere.
2. Determine the Pd/Pd<sub>4</sub>S phase boundary at low H<sub>2</sub> concentrations.
3. Test membrane in high-pressure feed streams with higher H<sub>2</sub> concentration.
4. Fabricate and evaluate tubular membrane.

All experimental milestones for FY 2007 were met using membranes that were developed at Argonne. In addition to meeting these milestones, we continued developing new membrane materials and fabrication methods to enhance the hydrogen flux of HTMs.

#### **IV. RESULTS**

Results obtained during FY 2007 are presented below in relation to the pertinent milestone. After discussing the work related to the milestones, work that was done outside the scope of the milestones is described.

##### **Milestone 1. Determine stability of membrane in steam-containing atmosphere.**

Because HTMs will encounter steam during operation, we studied the effect of water vapor on the hydrogen flux of an ANL-3e membrane (Pd/TZ-3Y, i.e., 50 vol.% Pd mixed with Y<sub>2</sub>O<sub>3</sub>-stabilized ZrO<sub>2</sub>) with a thickness of 0.22 mm. The disk-shaped membrane was sintered at  $1480^{\circ}\text{C}$  for 10 h in air, and then both faces were polished with 600-grit SiC paper. The hydrogen flux was measured at 600 and  $900^{\circ}\text{C}$  in tests using a sweep gas of ultra high purity (UHP) N<sub>2</sub> flowing at a constant rate of 150 cm<sup>3</sup>/min. Feed gas with a pH<sub>2</sub>O in the range 0.03-0.49 atm was obtained by bubbling mixtures of H<sub>2</sub> and He through a water bath (Fisher Scientific EX-35D1) at a temperature of 25-81°C. The H<sub>2</sub> partial pressure in the feed gas was kept constant (0.5 atm) by using mass flow controllers to adjust the flow rates of H<sub>2</sub> and He.

Figure 1 shows the hydrogen flux versus  $p_{\text{H}_2\text{O}}$  in the feed gas at 600 and 900°C. Each point for moist feed (i.e., 0.03, 0.07, 0.18, and 0.49 atm  $\text{H}_2\text{O}$ ) is the average of three or four separate measurements that were made over a period of 0.5-1.0 h, during which time the hydrogen flux showed no significant change. Although 0.5-1.0 h is a relatively brief period, it is expected that an ongoing reaction of the membrane would cause a discernible change in the flux. Before each measurement in a moist condition, the flux was measured in dry feed gas to confirm that the previous exposure to moisture had not irreversibly changed the membrane. The points for dry feed gas are the average of all flux values that were measured before and after each exposure to moisture at 600 and 900°C. The "dry" flux values at both temperatures showed good reproducibility. The reproducibility of flux values measured in dry gas and the steadiness of values measured in "moist" conditions suggest that the membrane is stable during short exposures to moisture (up to 0.49 atm  $\text{H}_2\text{O}$ ). Longer-term stability was tested at 500, 700, and 800°C using an ANL-3e membrane (thickness = 0.15 mm) in feed gas that was composed of 50%  $\text{H}_2$ /2%  $\text{H}_2\text{O}$ /balance He. Figure 2 shows that the flux was stable for >150 h at each of these temperatures.

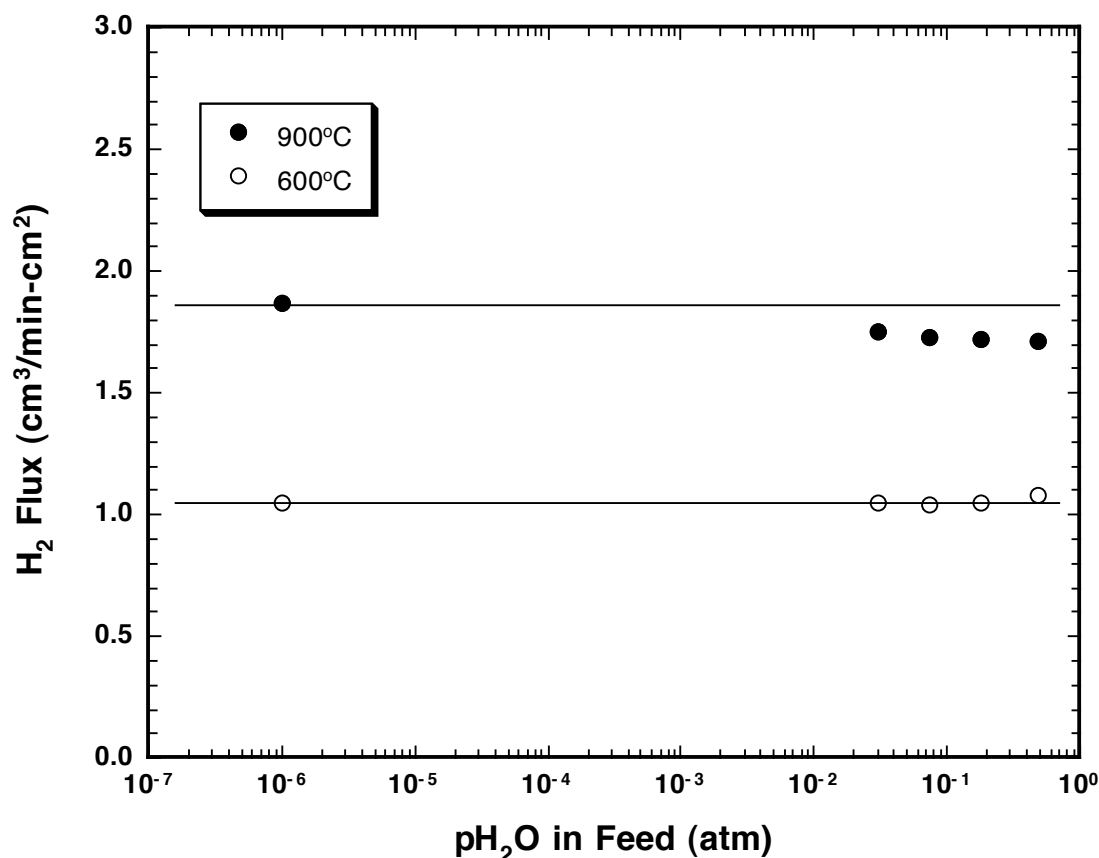


Fig. 1 Water-vapor pressure dependence of  $\text{H}_2$  flux at 600 and 900°C for ANL-3e membrane ( $\approx 0.22$ -mm thick).

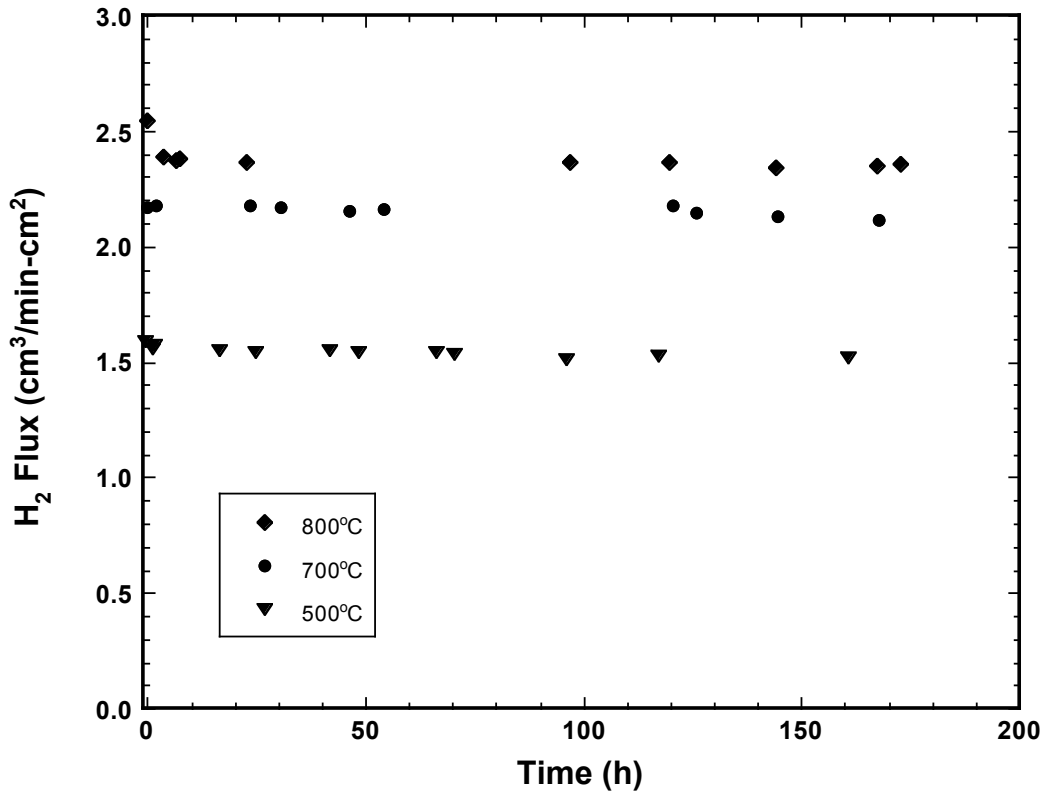


Fig. 2 Time dependence of  $H_2$  flux for 0.15-mm-thick ANL-3e membrane using 50%  $H_2$ /2%  $H_2O$ /balance He as feed gas.

The hydrogen flux was independent of  $p_{H_2O}$  in feed gas at 600°C (Fig. 1) but showed a slight systematic decrease versus  $p_{H_2O}$  in feed gas at 900°C. The decrease at 900°C is probably not due to water vapor creating a barrier to  $H_2$  absorption by occupying absorption sites, because a similar decrease would be evident at 600°C if this were the case. Oxygen diffusion through TZ-3Y, a component of the membrane and a known oxygen ion conductor, might explain the decrease in hydrogen flux at 900°C. Oxygen that is produced by water dissociation in the feed gas could permeate to the sweep side of the membrane, where it would react with permeated hydrogen. In addition, the diffusion of oxygen ions through TZ-3Y would be coupled with the diffusion of electrons through Pd, which might impede the permeation of hydrogen. Due to the thermally activated nature of oxygen permeation, these effects would be expected to influence the hydrogen flux more at 900°C than at 600°C.

After testing ANL-3e membranes in feed gas containing just hydrogen and steam, their stability was tested with a feed gas whose composition resembled "real-life" more closely. Figure 3 plots the hydrogen flux at 600-900°C for an  $\approx 0.27$ -mm-thick ANL-3e membrane in tests using simulated "syngas" as the feed gas. The composition of the feed gas was 52.7%  $H_2$ /20.6%  $H_2O$ /10.1% CO/8.0%  $CO_2$ /0.6%  $CH_4$ /balance He. The initial values were measured in dry syngas, and then moisture was added by bubbling the syngas through water at a temperature of  $\approx 61^\circ\text{C}$ . When moisture was added at 600 and

700°C, the flux initially increased slightly and then remained stable for >100 h. There was also a slight initial increase in the flux during tests at 800 and 900°C, but the flux decreased very slightly over longer times. Longer-term (100-1000 h) exposures at 800 and 900°C are needed to determine whether the flux continues to decrease or reaches a constant value. Calculation of the equilibrium gas compositions (Fig. 4) suggests that the initial increase in flux at each temperature resulted from an increase in hydrogen concentration in the feed gas. The fact that the flux remained stable at 600-700°C after an initial small increase indicates that the membrane is stable under these conditions. Longer-term studies will be necessary to evaluate the long-term stability at 800-900°C.

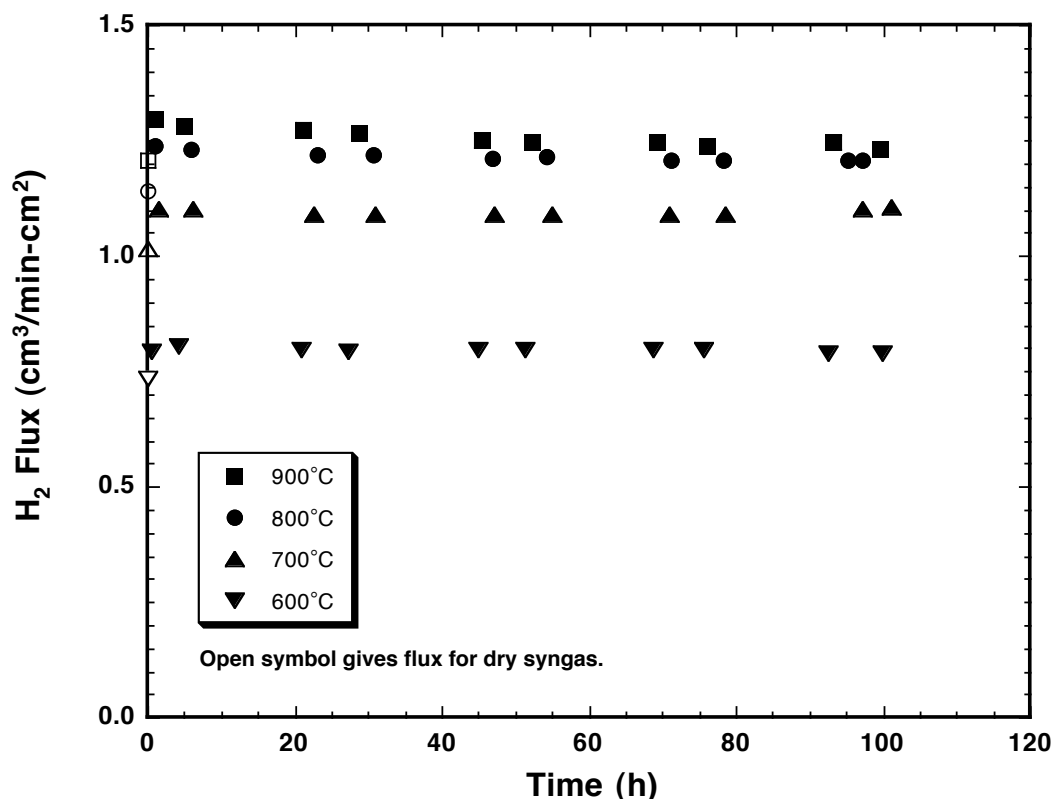


Fig. 3 Time dependence of hydrogen flux for 0.27-mm-thick ANL-3e membrane at 600-900°C using feed gas initially composed of dry 52.7%  $H_2$ /10.1%  $CO$ /8.0%  $CO_2$ /0.6%  $CH_4$ /balance He and then 52.7%  $H_2$ /20.6%  $H_2O$ /10.1%  $CO$ /8.0%  $CO_2$ /0.6%  $CH_4$ /balance He.

In another experiment, the hydrogen flux of an ANL-3e membrane was measured at 400-900°C in tests using a feed gas composed of  $\approx 50\%$   $CO$ /balance  $H_2O$ . In this experiment, feed gas was produced by bubbling 100% carbon monoxide through a water bath at  $\approx 81^\circ C$ , and hydrogen was produced via the water-gas shift reaction:



The hydrogen concentration was measured on both the feed and the sweep side of the membrane. Figure 5 plots the hydrogen flux through the membrane, and Fig. 6 shows the total hydrogen production rate (i.e., on both the feed and sweep sides of the membrane).

The hydrogen flux was low, because the membrane was relatively thick (0.27 mm) and the hydrogen concentration in the feed gas was low (<0.1% at 400°C and <3% at 900°C). The large difference between the measured and calculated equilibrium values for the total hydrogen production rate (Fig. 6) indicates that the reaction conditions were far from optimum. To increase the hydrogen production rate, the membrane thickness must be decreased and the residence time of the feed gas should be increased; nevertheless, these preliminary results indicate that the ANL-3e membrane functions as expected under conditions for the water-gas shift reaction.

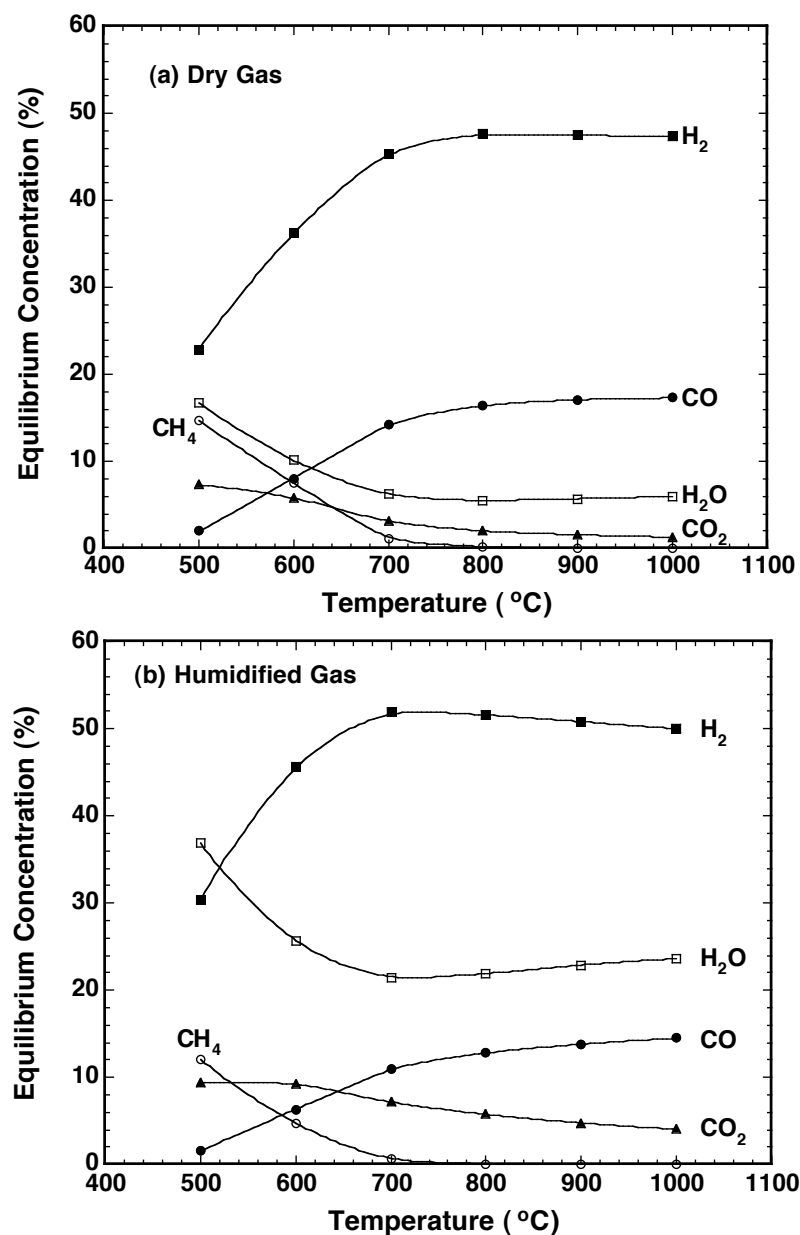


Fig. 4 Calculated equilibrium composition for (a) dry gas containing 52.7% H<sub>2</sub>/10.1% CO/8.0% CO<sub>2</sub>/0.6% CH<sub>4</sub>/balance He and (b) humidified gas containing 52.7% H<sub>2</sub>/20.6% H<sub>2</sub>O/10.1% CO/8.0% CO<sub>2</sub>/0.6% CH<sub>4</sub>/balance He.

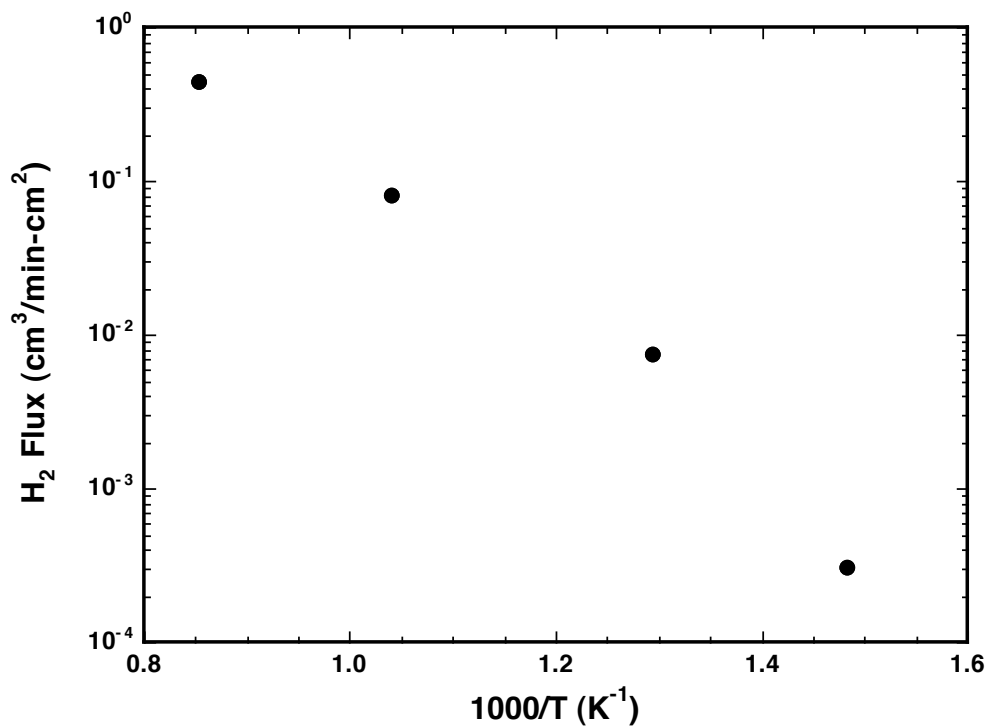


Fig. 5 Hydrogen flux through 0.27-mm-thick ANL-3e membrane using 50% CO/balance H<sub>2</sub>O as feed gas.

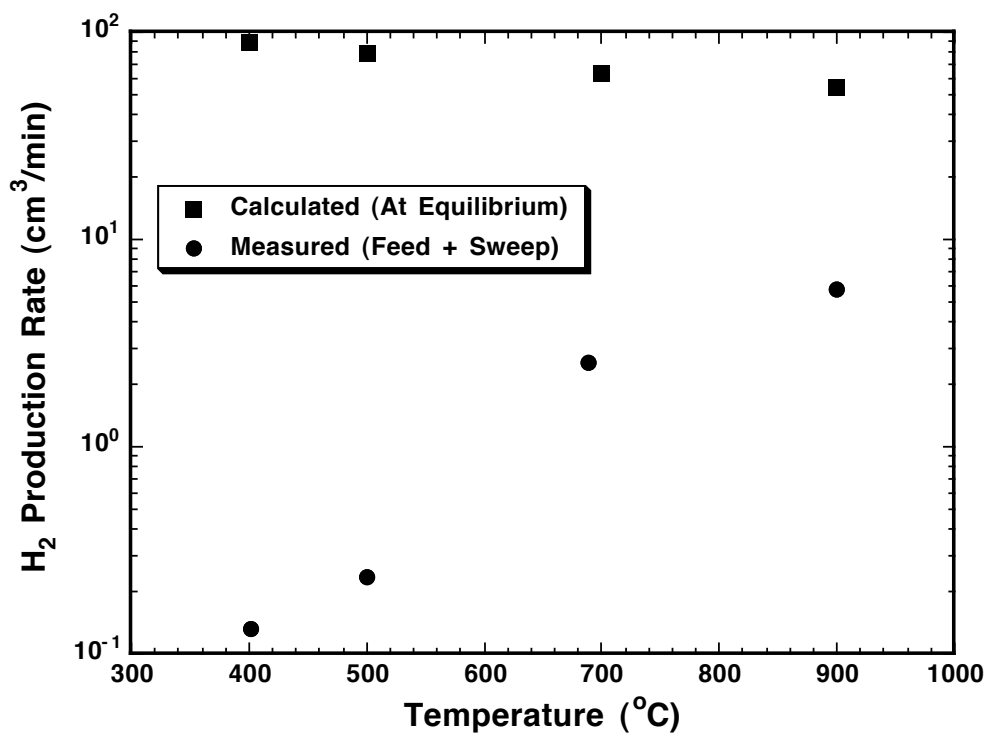


Fig. 6 Total hydrogen production rate (i.e., sum of production rate on feed and sweep side) of 0.27-mm-thick ANL-3e membrane using 50% CO/balance H<sub>2</sub>O as feed gas. HSC software was used to obtain the calculated (equilibrium) values.

## Milestone 2. Determine the Pd/Pd<sub>4</sub>S phase boundary at low H<sub>2</sub> concentrations.

Previous work [1] identified the position of the Pd/Pd<sub>4</sub>S phase boundary in gases that contained 73% H<sub>2</sub>. Because the H<sub>2</sub> concentration affects the position of the phase boundary [1], we determined in FY 2007 the Pd/Pd<sub>4</sub>S phase boundary in tests using feed gas with 10% H<sub>2</sub>. For these tests, we mixed TZ-3Y (i.e., ZrO<sub>2</sub> partially stabilized with Y<sub>2</sub>O<sub>3</sub>) powder from Tosoh Ceramics with Pd powder (50 vol.%) from Technic, Inc. ANL-3e membrane samples were made by uniaxially pressing the Pd/TZ-3Y mixture into disks, and then sintering the disks at 1400-1500°C for 5-10 h in ambient air.

The Pd/Pd<sub>4</sub>S phase boundary was determined in a feed gas mixture composed of 10% H<sub>2</sub>/8-50 ppm H<sub>2</sub>S/balance He. Mass flow controllers (MKS 1179A) were used to blend appropriate gases. The total flow rate of the mixture was 200 cm<sup>3</sup>/min, and the chamber holding the sample had a volume of  $\approx 2600$  cm<sup>3</sup>; therefore, a volume of gas equivalent to the volume of the sample chamber flowed in  $\approx 13$  min, and the gas composition in the sample chamber equaled the expected composition within  $\approx 1$  h of starting the flow of the gas mixture.

The ANL-3e samples were equilibrated for 48 h at selected temperatures in feed gas composed of 10% H<sub>2</sub>/8-50 ppm H<sub>2</sub>S/balance He. After each equilibration, the surface of the sample and a polished cross section were examined with a JEOL 5400 scanning electron microscope (SEM) to determine whether Pd<sub>4</sub>S had formed. Energy dispersive spectroscopy (EDS) for chemical analysis of microstructural features was done with a Voyager system (Thermo Electron). Equilibrations were done by heating at 180°C/h in flowing He and then switching to a feed gas of 10% H<sub>2</sub>/8-50 ppm H<sub>2</sub>S/balance He after the sample reached the selected temperature. When the sample had been held for 48 h at the selected temperature, the feed gas was switched back to He, the sample was held for an additional 6 h, and then it was cooled in flowing He at a rate of 180°C/h.

Figure 7 shows the Pd/Pd<sub>4</sub>S phase boundary that was determined by experiments at Argonne and by calculation using thermodynamic data for the Pd-S system [2] and the H<sub>2</sub>/S<sub>2</sub>/H<sub>2</sub>S equilibrium [3]. Each calculated point is a temperature at which Pd and Pd<sub>4</sub>S are in equilibrium for given H<sub>2</sub> and H<sub>2</sub>S concentrations; at higher temperature, Pd is stable and Pd<sub>4</sub>S unstable, whereas Pd<sub>4</sub>S is stable and Pd unstable at lower temperature. Points were calculated for gas with 73% H<sub>2</sub> and with 10% H<sub>2</sub> to illustrate the effect of hydrogen concentration on the phase boundary (through the H<sub>2</sub>/S<sub>2</sub>/H<sub>2</sub>S equilibrium). Points with bars were determined at Argonne by examining ANL-3e samples after they were equilibrated in H<sub>2</sub>/H<sub>2</sub>S mixtures [1], and include new results that were obtained in tests using feed gas with 10% H<sub>2</sub>/8-50 ppm H<sub>2</sub>S/balance He. The low-temperature end of the bar represents the highest temperature at which Pd<sub>4</sub>S was found after an equilibration; the high-temperature end gives the lowest temperature at which Pd was stable; the Pd/Pd<sub>4</sub>S phase boundary lies somewhere between these two temperatures. For example, the phase boundary for ANL-3e membranes exposed to 10% H<sub>2</sub>/8 ppm H<sub>2</sub>S/balance He lies in the range 450-475°C.

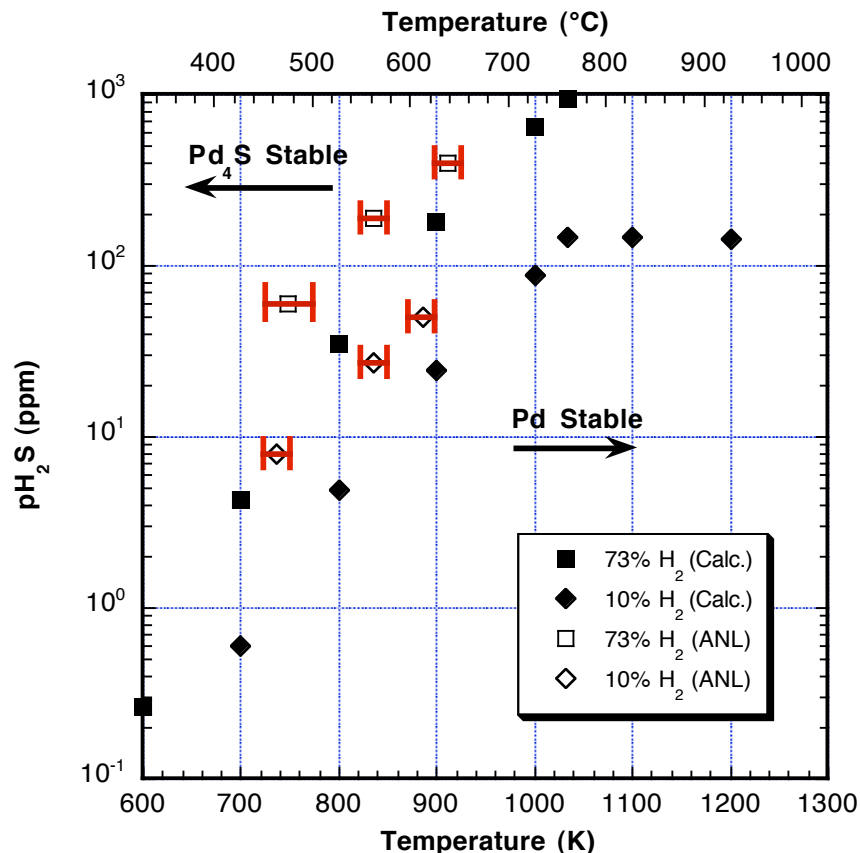


Fig. 7 Partial pressure for  $H_2S$  vs. temperature illustrating Pd/Pd<sub>4</sub>S phase boundary for gases containing 73% and 10%  $H_2$ . Calculated using data from literature [2, 3] or determined at Argonne by equilibrating samples at various temperatures and then examining for evidence of reaction.

The Argonne data for the Pd/Pd<sub>4</sub>S phase boundary (Fig. 7) show that the ANL-3e membranes are stable in feed gas of 10%  $H_2$ /50 ppm  $H_2S$ /balance He at temperatures above  $\approx 625^\circ\text{C}$ . At lower temperatures, Pd<sub>4</sub>S forms on the surface of the membrane and impedes hydrogen permeation. Formation of Pd<sub>4</sub>S would not necessarily render the membrane useless, however, if the Pd<sub>4</sub>S layer is not too thick and its permeability is not too low. In addition, we showed earlier that membranes can in some cases be regenerated after they react with  $H_2S$  [1]. While the phase boundary lies at  $\approx 625^\circ\text{C}$  for feed gas with 10%  $H_2$  and 50 ppm  $H_2S$ , it shifts to significantly lower temperature ( $\approx 450^\circ\text{C}$ ) in feed gas with the same  $H_2S$  concentration but with 73%  $H_2$ , because the phase boundary depends on the  $H_2$  as well as the  $H_2S$  concentration.

For both 10% and 73%  $H_2$ , the phase boundary determined at Argonne is at lower temperature than the boundary calculated from thermodynamic data [2, 3]. Considering that the thermodynamic data for the calculated boundary were extrapolated from higher temperatures ( $\approx 675$ - $780^\circ\text{C}$ ), the discrepancy in the results is not large. Based on this small difference, we speculated [4] that the ceramic matrix might stabilize Pd slightly against reaction with  $H_2S$  in the way that acidic catalyst supports increase the sulfur



tolerance of Pd-Pt catalysts [5, 6]. To test this hypothesis, we included Pd foil along with ANL-3e samples during equilibrations at 500-600°C in 10% H<sub>2</sub>/27 ppm H<sub>2</sub>S/balance He and at 600-650°C in 10% H<sub>2</sub>/50 ppm H<sub>2</sub>S/balance He. In all cases, the results were identical for foil and membrane samples, indicating that the ceramic matrix does not stabilize Pd under these conditions.

To extract thermodynamic parameters from our phase boundary data, we considered the following reactions:



Using the reactions in Eqns. 2-4, we derived the following relationship between  $K_2$ , the equilibrium constant for reaction (2), and the values of temperature,  $p\text{H}_2$ , and  $p\text{H}_2\text{S}$  for points on the phase boundary:

$$-RT \ln K_2 = -RT \ln (p\text{H}_2/p\text{H}_2\text{S}) - \Delta G_3^\circ \quad (5)$$

where  $p\text{H}_2$  and  $p\text{H}_2\text{S}$  are the partial pressures given by the feed gas composition;  $\Delta G_3^\circ$ , the standard free energy of formation for reaction (3), is taken from Knacke et al. [3]; and the temperature  $T$  is taken from Fig. 7. Using Eqn. (5), we plot  $\ln K_2$  vs. inverse temperature (Fig. 8), which can be used to predict the phase boundary versus temperature and feed gas composition ( $p\text{H}_2/p\text{H}_2\text{S}$ ).

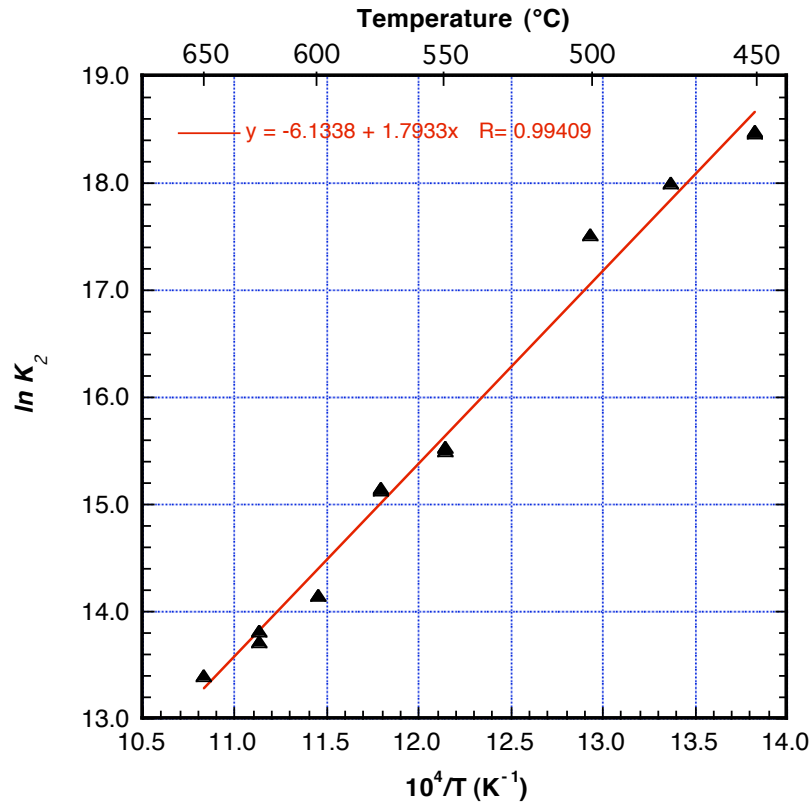


Fig. 8 Equilibrium constant for reaction (2), calculated using Eqn. (5) and experimental data (i.e., bars in Fig. 7) determined at Argonne.

Because Fig. 7 gives a range of temperatures in which the phase boundary lies for a given feed gas composition, rather than a specific temperature, Fig. 8 includes the low- and high-temperature ends of the bars from Fig. 7. Figure 9 shows phase boundaries that were calculated for feed gas with 73% and 10%  $H_2$  along with experimental points that were taken from Fig. 7 for the same feed gas compositions. Using Fig. 8, we calculated the standard free energy of formation for reaction (2),  $\Delta G_2^\circ$ , and compared our values to those reported by Taylor [2]. As seen in Table 1, the difference in  $\Delta G_2^\circ$  values is not large, Argonne's values differing from Taylor's by only  $\approx 5$ -10%. Nevertheless, the difference is large enough to account for the shift in the phase boundary seen in Fig. 7.

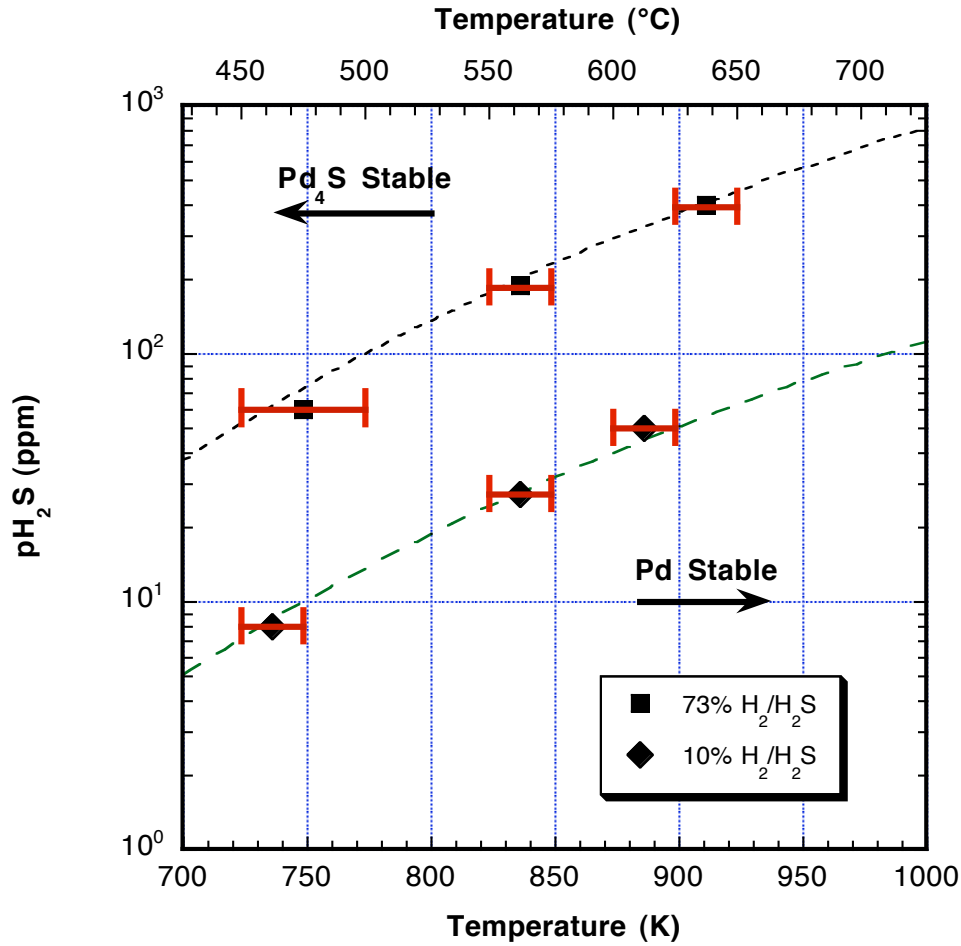


Fig. 9 Partial pressure for  $H_2S$  vs. temperature illustrating  $Pd/Pd_4S$  phase boundary for gases containing 73% and 10%  $H_2$ . Lines were calculated using fit of data in Fig. 8; bars are reproduced from Fig. 7 and represent Argonne experimental data.

*Table 1 Free energy of formation for Pd<sub>4</sub>S (reaction 2) calculated from Argonne's data (Fig. 7) and from Taylor (Ref. 2)*

Feed Gas	Phase Boundary (°C)	$\Delta G_2^\circ$ (Argonne) (kJ/mol)	$\Delta G_2^\circ$ (Taylor) (kJ/mol)
73% H <sub>2</sub> /400 ppm H <sub>2</sub> S	T(Low) = 625	-102	-109
	T(High) = 650	-103	-107
73% H <sub>2</sub> /191 ppm H <sub>2</sub> S	T(Low) = 550	-106	-115
	T(High) = 575	-107	-113
73% H <sub>2</sub> /59 ppm H <sub>2</sub> S	T(Low) = 450	-111	-124
	T(High) = 500	-113	-119
10% H <sub>2</sub> /50 ppm H <sub>2</sub> S	T(Low) = 600	-103	-111
	T(High) = 625	-103	-109
10% H <sub>2</sub> /27 ppm H <sub>2</sub> S	T(Low) = 550	-106	-115
	T(High) = 575	-107	-113
10% H <sub>2</sub> /8 ppm H <sub>2</sub> S	T(Low) = 450	-111	-124
	T(High) = 475	-112	-121

**Milestone 3. Test membrane in high-pressure feed streams with higher H<sub>2</sub> concentration.**

Using Argonne's high-pressure reactor, we measured the hydrogen flux through a disk-shaped ANL-3e sample at temperatures up to 900°C and pressures up to 280 psig using a feed gas of 4% H<sub>2</sub>/balance He [1]. This report presents results obtained during FY 2007 at Argonne in tests using a feed gas of 90% H<sub>2</sub>/balance He at temperatures up to 900°C and pressures up to 300 psig.

The hydrogen flux through an ANL-3e membrane was measured for a disk-shaped sample ( $\approx 0.86$ -mm thick x  $\approx 20$ -mm diameter) that was made by uniaxially hot-pressing a Pd/TZ-3Y powder mixture at 1250°C for 25 min. The powder mixture for the membrane was prepared by mixing TZ-3Y (i.e., ZrO<sub>2</sub> partially stabilized with Y<sub>2</sub>O<sub>3</sub>) powder from Tosoh Ceramics with Pd powder (50 vol.%) from Technic, Inc.

Both sides of the sample were polished with 600-grit SiC polishing paper, and the sample was sealed between two high-strength Haynes HR-160 tubes by means of graphite gaskets in a VCR-type fitting.

The feed gas composition was 90% H<sub>2</sub>/balance He, and the sweep gas composition was 100 ppm H<sub>2</sub>/balance N<sub>2</sub>. The hydrogen flux was measured at 500°C in  $\approx 75$ -psi increments up to a total pressure of  $\approx 300$  psig in both the feed and sweep gases. While maintaining the total pressure at  $\approx 300$  psig, we measured the flux in  $\approx 100^\circ\text{C}$  increments up to  $\approx 900^\circ\text{C}$ . Shortly after the sample reached 900°C and 300 psig, the seal on the feed side of the sample began to leak; therefore, all subsequent measurements had to be made at lower pressures ( $< 100$  psig).

For each reported value of hydrogen flux, the hydrogen and helium concentrations in the sweep stream were measured at least four times by using a Hewlett-Packard 6890 gas chromatograph. While measurements were being made, the total pressures in the feed and sweep streams differed by <5 psi. To calculate the hydrogen flux, the measured  $H_2$  concentration in the sweep stream was corrected for the initial  $H_2$  concentration in the sweep stream (100 ppm) and for leakage (based on the measured helium leakage rate).

Figure 10 plots hydrogen flux values that were measured at 500-900°C versus  $\Delta p H_2^{1/2}$ , which is defined in terms of the partial pressures of hydrogen on the feed and sweep sides of the membrane:

$$\Delta p H_2^{1/2} \equiv \sqrt{p H_2(\text{feed})} - \sqrt{p H_2(\text{sweep})} \quad (6)$$

Argonne's recent data are shown by solid symbols, whereas data collected previously at NETL [1] are shown by open symbols. As expected for hydrogen diffusion through a metal, the flux at each temperature varies linearly with  $\Delta p H_2^{1/2}$ .

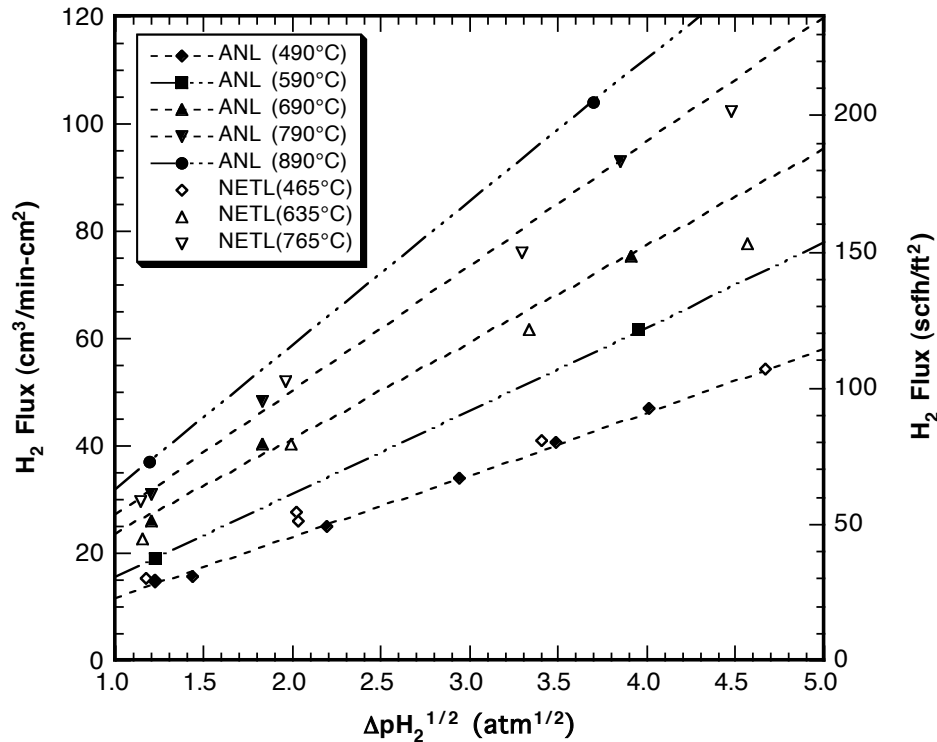


Fig. 10 Hydrogen flux vs.  $\Delta p H_2^{1/2}$  (defined in text) for ANL-3 membranes tested in high-pressure reactors at Argonne and NETL. All values are normalized for a membrane thickness of 20  $\mu m$ .

The slope increases as temperature increases because it is directly related to the membrane's thermally activated hydrogen permeability. The maximum value of  $\Delta p H_2^{1/2}$  decreases as temperature increases (e.g., 4.0 at 490°C vs. 3.7 at 890°C), because  $p H_2(\text{sweep})$  increases as the hydrogen flux increases, while  $p H_2(\text{feed})$  is fixed by the maximum allowable pressure for the experiment (300 psig). Flux values from Argonne and NETL agree in general, but Argonne's values are shifted  $\approx 25^\circ C$  relative to NETL's values (e.g., Argonne's values at 490°C agree well with NETL's values at 465°C).

Figure 11 compares hydrogen flux values measured in Argonne's high-pressure reactor, Argonne's ambient-pressure reactor [7], and NETL's high-pressure facility [7]. The hydrogen partial pressure was varied in the ambient-pressure reactor by changing the composition of the feed gas while maintaining a total pressure of 15 psi (1 atm), whereas it was varied in the high-pressure reactors at Argonne and NETL by changing the total pressure while fixing the composition of the feed gas at 90% H<sub>2</sub>/balance He. In Fig. 11, all flux values measured in the high-pressure reactors are normalized for a membrane sample thickness of 20  $\mu\text{m}$ . The dashed lines show linear fits of the data measured at ambient pressure and temperatures of 600°C and 900°C, and are provided mainly as guides to the eye. The values measured in Argonne's high-pressure reactor are consistent with those measured previously at Argonne at ambient pressure and at NETL at high pressure. This agreement suggests that the values obtained with Argonne's high-pressure reactor are reasonable.

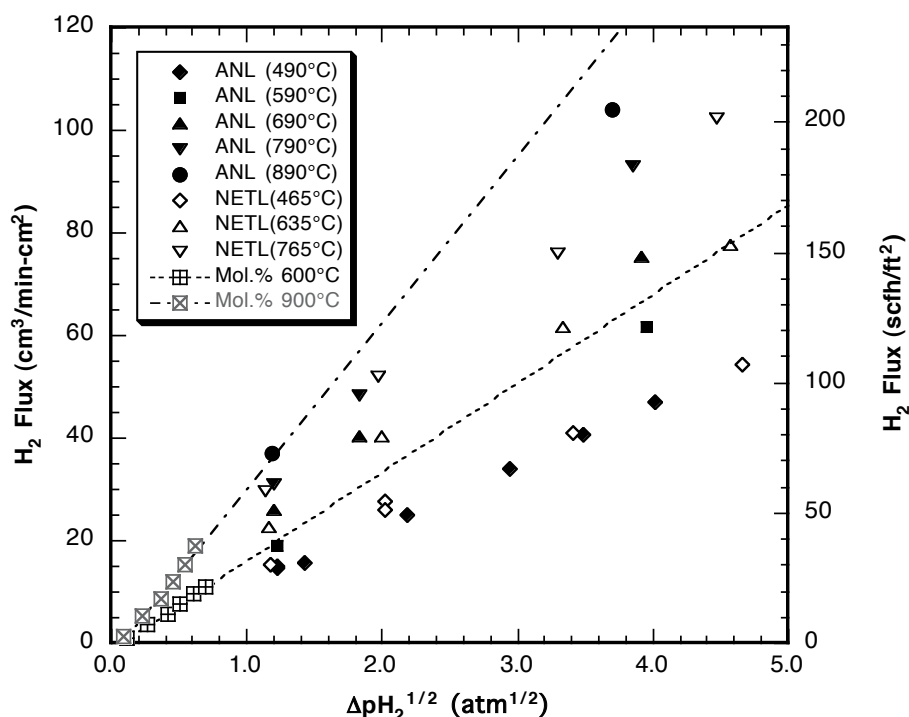
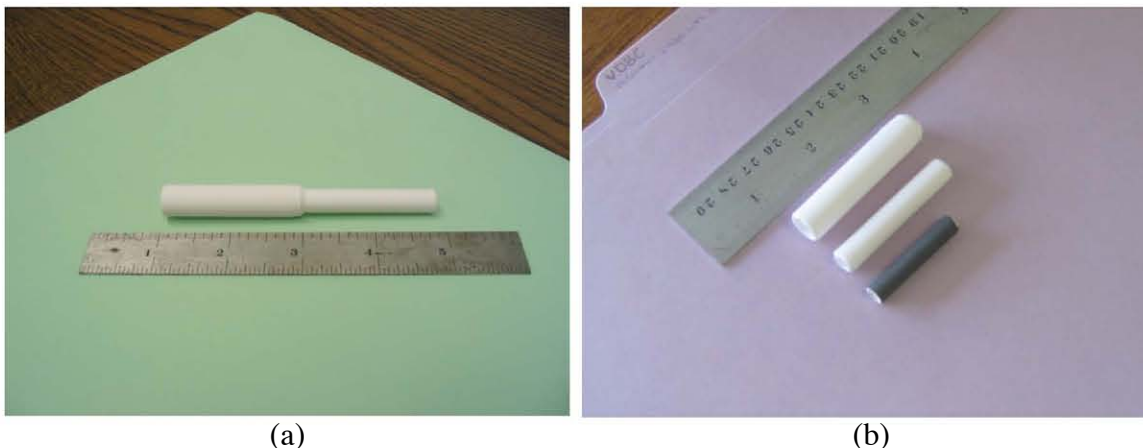


Fig. 11 Hydrogen flux of ANL-3 membranes measured by varying  $p H_2$  in high-pressure reactors at Argonne and NETL [7] and by varying  $H_2$  content (mol.%) in Argonne's ambient-pressure reactor. All values are normalized for a membrane thickness of 20  $\mu\text{m}$ .

The high-pressure reactor will be used in several future investigations. Measurements made at NETL [1] indicated that the measured hydrogen permeability for the ANL-3e membrane increased as the sweep gas flow rate increased, possibly due to concentration polarization at low flow rates. Based on these results, we will investigate the effects of gas (sweep and feed) flow rates on hydrogen flux. We will also measure the hydrogen flux while imposing a gradient in total pressure across the sample rather than a gradient in hydrogen partial pressure, as was done in gathering data (Fig. 10) for this report, and we will study the effects of cycling pressure and temperature on the hydrogen flux of ANL-3 membranes.

#### Milestone 4. Fabricate and evaluate tubular membrane.

To be practical, HTMs must be available in a shape that has a large active area, such as tubes; therefore, we began to develop methods for fabricating tubular membranes during FY 2007. In one approach, we are adapting the paste-painting technique that has been used to fabricate disk-shaped ANL-3e thin films. In this approach, we first produce porous alumina support tubes in a cold isostatic press (Engineered Pressure Systems) by pressing alumina hydrate powder in a rubber mold (Trexler Rubber) with a stainless steel mandrel at 10,000-15,000 psig. After pressing, tubes are pre-sintered in air for 3-5 h at 800-950°C. Figure 12a shows a photograph of such a tube. After the tube is pre-sintered, its outside surface is painted with a slurry of ANL-3e components and is then sintered at 1400-1500°C for 5 h in air. Figure 12b shows a photograph of two porous alumina support tubes next to an ANL-3e film that was sintered on a tubular porous alumina support. Tubes presently being produced are typically 8-10 cm in length with an outside diameter of  $\approx 1$  cm and a membrane thickness of 25-50  $\mu\text{m}$ .



*Fig. 12 a) Porous alumina tube after pre-sintering for 5 h at 700-800°C in air and b) two porous alumina tubes and ANL-3e film on porous alumina tube after sintering for 5 h at 1400°C in air.*

Tubular thin films are tested for pinholes and/or microcracks by checking for penetration of the film by isopropyl alcohol (IPA). In this test, the tube is filled with IPA, and the tube is examined for evidence that IPA is penetrating the film on its outer surface. Penetration of the film by even a small amount of IPA is visible as a darkening of the film and indicates that the membrane film contains cracks or interconnected porosity. An IPA-penetration test of the tube coated with an ANL-3e film (Fig. 12b) showed that some areas were porous, probably because the slurry had been painted on too thinly.

If an IPA-penetration test reveals no leakage, we then measured the tube's hydrogen flux in a spring-loaded test fixture like that shown in Fig. 13. With this fixture, graphite gaskets are placed on the ends of the tube, and the tube and gaskets are squeezed between an alumina tube and an alumina plate. To achieve a leak-tight seal, the open ends of the tube are polished so they are flat and perpendicular to the axis of the tube. When the pre-sintered support tube is coated with membrane material, the paste for making the membrane film is painted onto the entire outer surface of the support tube, including the open end, to improve the seal at the ends of the tube.

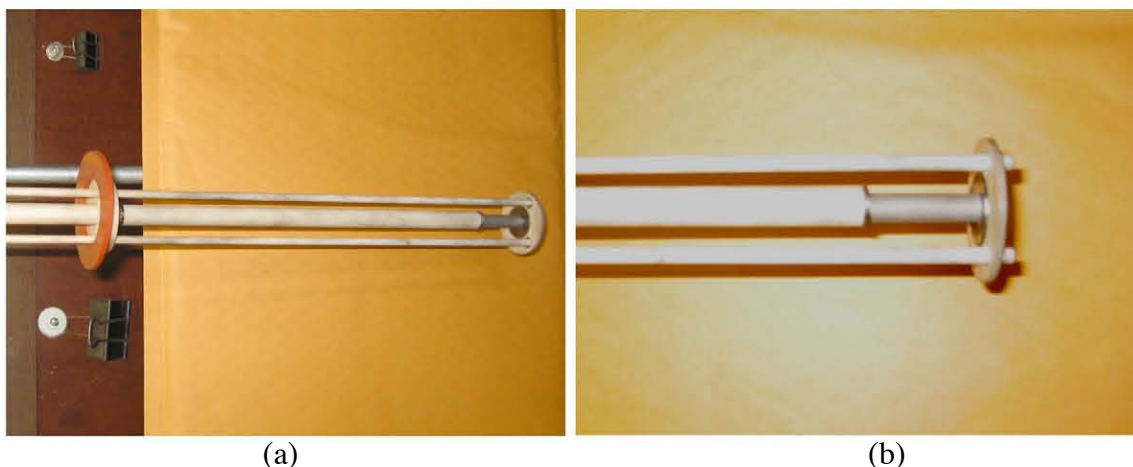


*Fig. 13 Porous alumina tube coated with dense ANL-3e film on spring-loaded fixture used to measure tube's hydrogen flux.*

After a tube passes the IPA test, it is sealed to a spring-loaded fixture and checked for leakage at room temperature, which is done by pressurizing the tube with 5 psi He and then submerging it in IPA. If bubbles are not observed through the wall of the painted tube, and if bubbling is minimal at the graphite gasket between the membrane tube and the test fixture, the tube is placed into the reactor to measure its hydrogen flux. It is then heated to 500°C while flowing helium on its feed side and N<sub>2</sub> on its sweep side at a rate of 150 ml/min. The hydrogen flux and permeability are measured with the hydrogen concentration in the sweep gas being corrected for leakage based on the measured leakage of helium.

Figure 14 shows the hydrogen flux and Fig. 15 the hydrogen permeability versus temperature (500-900°C) for a tubular HTM. The tube consisted of an ANL-3 thin film [Pd (60 vol.%)/CeO<sub>2</sub>, thickness  $\approx 30$   $\mu\text{m}$ ] on porous Al<sub>2</sub>O<sub>3</sub> and had a length of 8.03 cm and outside diameter of 0.85 cm. The feed gas contained either 90% H<sub>2</sub>/balance He or 4% H<sub>2</sub>/balance He. The flux (Fig. 14) and permeability (Fig. 15) values are low compared to values we have measured using disk-shaped samples that were either polished or consisted of thin films on porous disks.

We attribute this decline to several factors. First, CeO<sub>2</sub> was used as the ceramic component of the ANL-3 film because films containing CeO<sub>2</sub> attain high density during sintering. The tendency of CeO<sub>2</sub>-containing films to reach high density increases the likelihood that they will be free of leaks. However, we earlier found [8] that disk-shaped films made with CeO<sub>2</sub> have hydrogen flux values that are 15-40% lower than films made with TZ-3Y, even though the films made with TZ-3Y were 50% thicker. The CeO<sub>2</sub>-containing films might have low flux and permeability values because the Pd content on their surface is low [8], or because the increased density impedes hydrogen transport (if gas-phase transport in isolated pores contributes significantly to hydrogen transport). Although the explanation is unclear at this point, our data indicate that the performance of CeO<sub>2</sub>-containing films is inferior to that of films made with TZ-3Y or Al<sub>2</sub>O<sub>3</sub>.

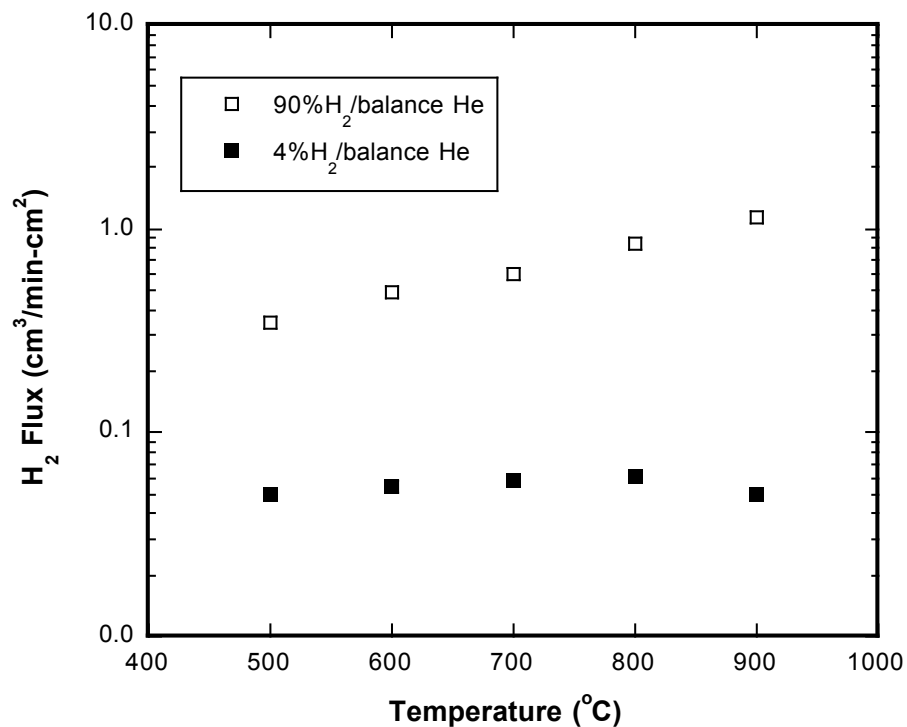


Fig. 14 Hydrogen flux for tubular ANL-3 thin film on porous  $\text{Al}_2\text{O}_3$ . Thin film contained Pd (60 vol.%)/ $\text{CeO}_2$  and had thickness of  $\approx 30 \mu\text{m}$ .

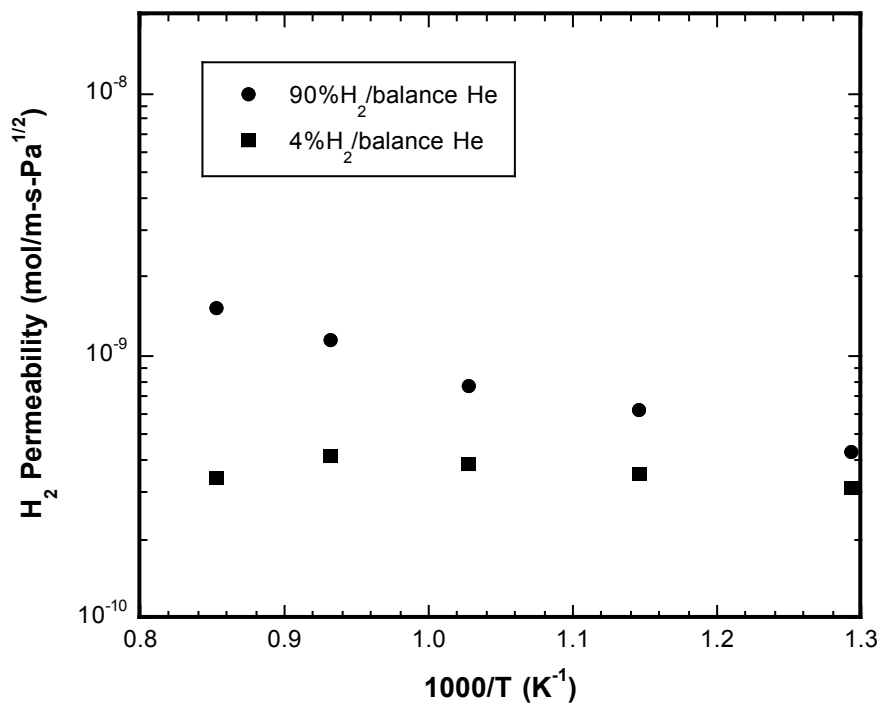
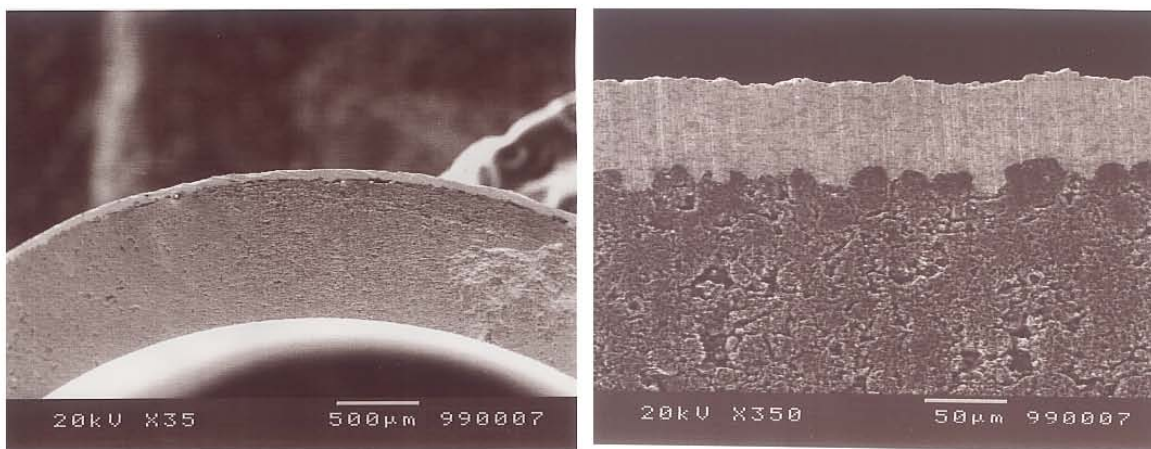


Fig. 15 Hydrogen permeability for tubular ANL-3 thin film on porous  $\text{Al}_2\text{O}_3$ . Thin film contained Pd (60 vol.%)/ $\text{CeO}_2$  and had thickness of  $\approx 30 \mu\text{m}$ .



Two observations suggest that the low flux and permeability values might also result partly from concentration polarization during the measurements. First, the flux and permeability are essentially independent of temperature when 4% H<sub>2</sub>/balance He is used as the feed gas, and second, the permeability depends strongly on the hydrogen concentration in the feed gas, especially at high temperatures. Concentration polarization might be expected to be more important for films made on tubular porous supports, because the porous support might facilitate the establishment of a boundary layer at the membrane surface.

Higher values of hydrogen flux and permeability were measured recently with another tubular HTM that consisted of a porous alumina tube coated with a thin film of Pd (60 vol. %)/TZ-3Y. The tube was closed on one end with a length of  $\approx 8.3$  cm and an outside diameter of  $\approx 1$  cm. Based on measurements made with an SEM, the thickness of the membrane film was  $58(\pm 4)$   $\mu\text{m}$ . Cross-sectional views of the tube after flux measurements are shown in Fig. 16. The dense HTM film was on the outside surface of the tube, and the relatively thick porous layer was on the inside. To investigate the possibility that concentration polarization influenced the results, the flow rates of the feed and sweep gases were varied in the range 150-500 ml/min. In addition, two flow patterns were used. In one pattern, feed gas flowed inside the tube while sweep gas on the outside of the tube; in the other pattern, feed gas flow was the opposite. The feed gas was composed of either 4% H<sub>2</sub>/balance He or 90% H<sub>2</sub>/balance He, while the sweep gas consisted of 100% N<sub>2</sub>.



*Fig. 16 Cross-sectional views of tubular Pd (60 vol. %)/TZ-3Y film (thickness  $\approx 58$   $\mu\text{m}$ ) on porous Al<sub>2</sub>O<sub>3</sub> tube. Tube's hydrogen flux and permeability values are given in Figs. 19 and 20.*

Figure 17 shows the effect of the gas flow pattern on the tube's hydrogen flux, and Fig. 18 shows the effect on its hydrogen permeability. The flow pattern has only a minimal effect on the flux and the permeability. Because the effect of flow pattern was negligible, the rest of the measurements were done in the normal flow pattern, in which feed gas flows on the outside of the tube and sweep gas on the inside.

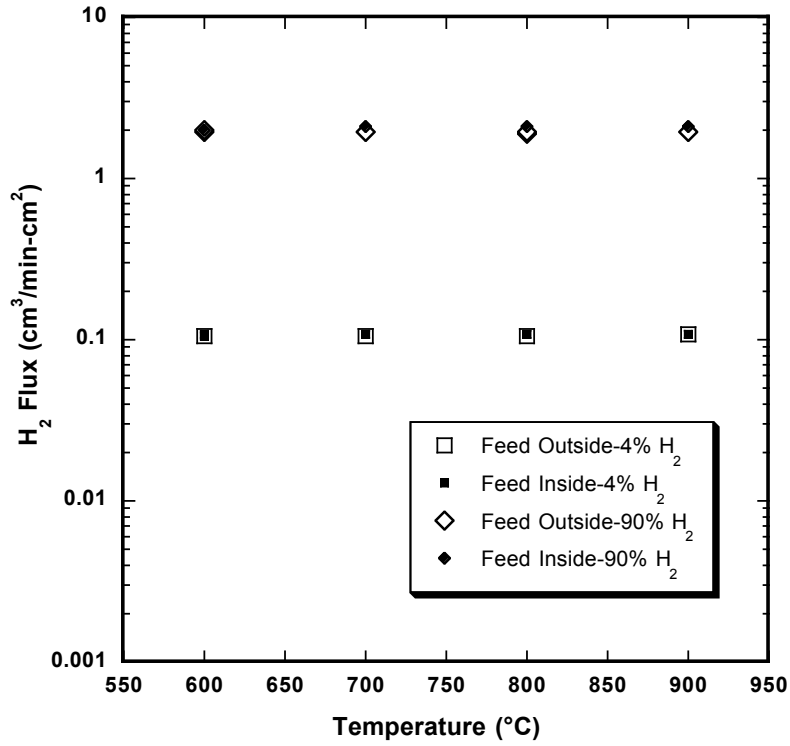


Fig. 17 Hydrogen flux for 58- $\mu$ m-thick Pd (60 vol.%) / TZ-3Y film on porous  $\text{Al}_2\text{O}_3$  measured with different flow patterns.

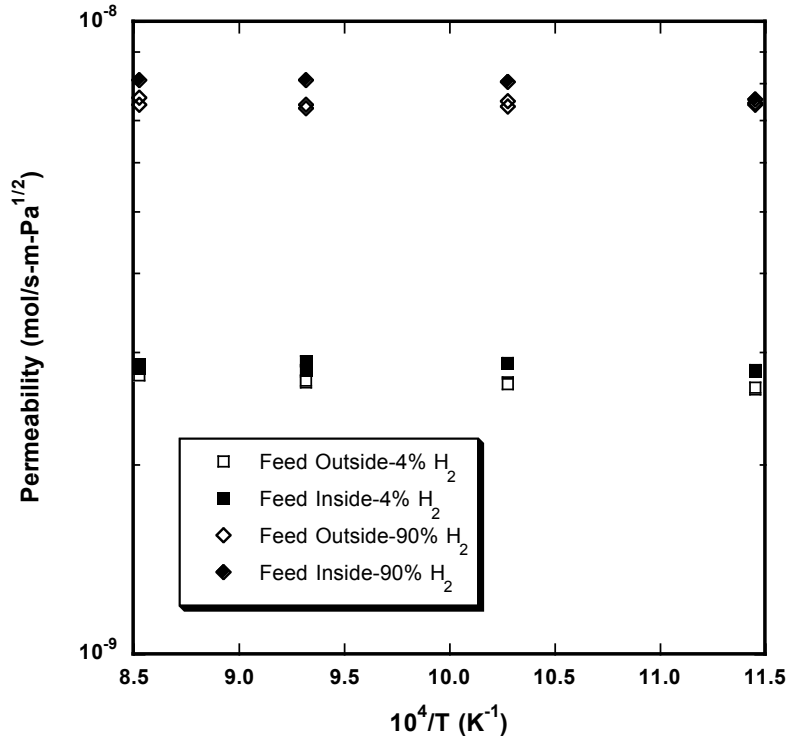


Fig. 18 Hydrogen permeability for 58- $\mu$ m-thick Pd (60 vol.%) / TZ-3Y film on porous  $\text{Al}_2\text{O}_3$  measured with different flow patterns.

Figure 19 shows the hydrogen flux values that were measured for the tube with a Pd/TZ-3Y film, and Fig. 20 shows the permeability values. The data are plotted as a function of temperature for different flow rates in the feed and sweep gases and different hydrogen concentrations in the feed gas. At every temperature, whether the feed gas contained 4% or 90% H<sub>2</sub>/balance He, the flux and permeability values for the tube made with Pd/TZ-3Y (Fig. 19 and 20) were several times larger than the values for the tube made with Pd/CeO<sub>2</sub> (Fig. 14 and 15), even though the Pd/TZ-3Y film was approximately twice as thick. We reported earlier [4] that Pd/TZ-3Y films also exhibited better performance than Pd/CeO<sub>2</sub> films on disk-shaped porous alumina supports. We are not certain why Pd/TZ-3Y films exhibit superior performance, but the performance of Pd/CeO<sub>2</sub> films might be degraded by evaporation of Pd during sintering, while the performance of Pd/TZ-3Y films might be enhanced by trapped porosity [4].

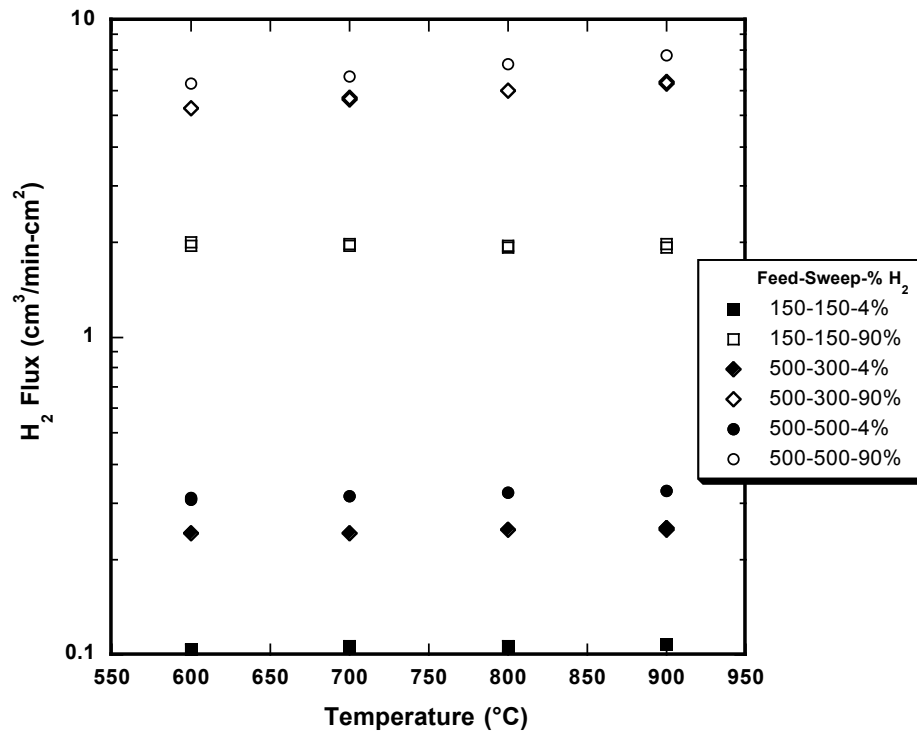


Fig. 19 Hydrogen flux for 58- $\mu$ m-thick Pd (60 vol.%) / TZ-3Y film on porous Al<sub>2</sub>O<sub>3</sub> tube measured with various gas flow rates (ml/min). Inset gives feed flow rate/sweep flow rate/H<sub>2</sub> concentration (%) in feed. Sweep was 100% N<sub>2</sub>.

The tube with Pd/TZ-3Y showed improved performance, compared to the tube made with Pd/CeO<sub>2</sub>, but effects from concentration polarization are still evident, especially for feed gas with 4% H<sub>2</sub> (at all flow rates tested) and 90% H<sub>2</sub> (at low sweep gas flow rate, 150 ml/min). The flux and permeability values are essentially independent of temperature under these conditions, and the permeability values are significantly lower than predicted from literature values for palladium [9]. Figure 20 shows a line that represents 60% of Koffler et al.'s permeability value for palladium [9]. Because Argonne's membrane contains 60 vol.% Pd, this line plots the "expected" permeability values for Argonne's membrane, if we assume concentration polarization does not affect

our values or the literature values. The significant difference between expected permeability values and Argonne's measured values indicates that concentration polarization is a factor for feed gas with 4% H<sub>2</sub> over a wide flow rate and feed gas with 90% H<sub>2</sub> at low gas flow rate.

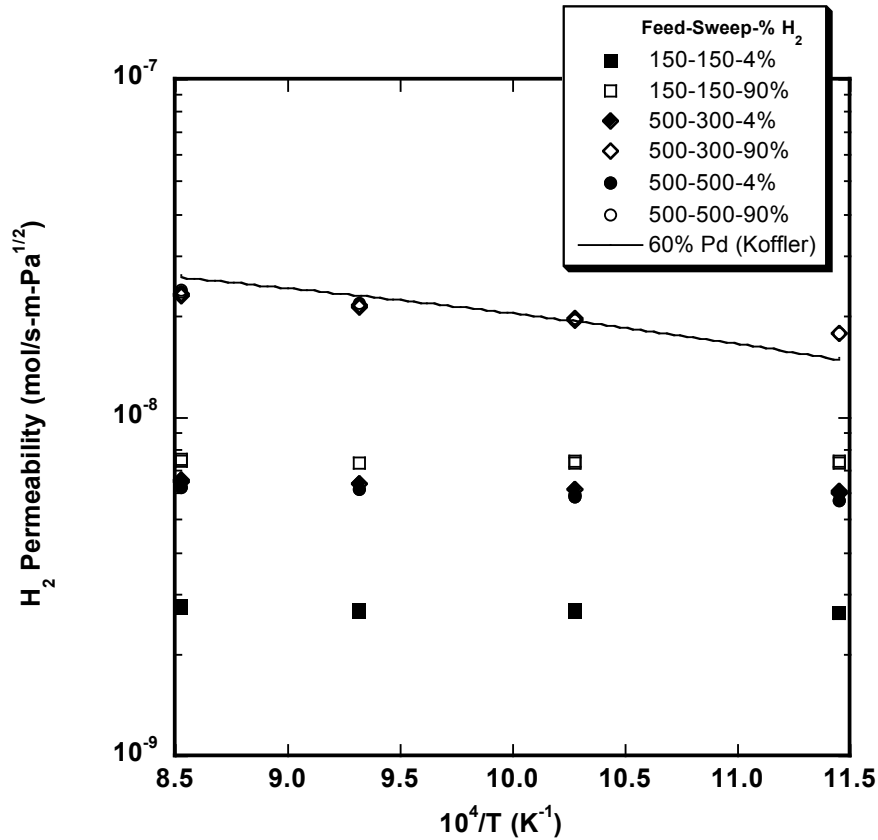


Fig. 20 Hydrogen permeability for 58- $\mu\text{m}$ -thick Pd (60 vol.%) / TZ-3Y film on porous Al<sub>2</sub>O<sub>3</sub> tube measured with various gas flow rates (ml/min). Legend gives feed flow rate/sweep flow rate/H<sub>2</sub> concentration (%) in feed. Sweep was 100% N<sub>2</sub>.

The effects from concentration polarization are largely overcome with high hydrogen concentration in the feed gas and high gas flow rates. Whether the feed gas contains 4% or 90% H<sub>2</sub>, the flux and permeability values increased significantly when the sweep flow rate increased from 150 to 300 ml/min and the feed flow rate increased from 150 to 500 ml/min. It is not clear whether the increase in measured values is related to polarization on the feed side or the sweep side of the membrane, because the feed and sweep flow rates were increased together. Even with high gas flow rates, however, the permeability values for feed gas with 4% H<sub>2</sub> are much smaller than the expected values, indicating that concentration polarization remains a factor for feed gas with low hydrogen concentration. By contrast, permeability values measured with 90% H<sub>2</sub> as the feed gas and sweep gas flow rate  $\geq 300$  ml/min were close to the expected values, and both flux and permeability increased with temperature, as expected due to the activated nature of hydrogen permeation. These results suggest that concentration polarization is minimized by high gas flow rates and high hydrogen concentration in the feed gas.

## V. FUTURE WORK

*Development of Tubular HTMs.* We will continue fabricating tubular HTMs to increase their effective area and demonstrate that they can be made into practical devices. These tubes can be fabricated as either monoliths, in which the entire tube is composed of HTM components, or as thin films on porous tubular supports. We will focus on fabricating HTM thin films on porous supports, because they have produced promising results. Paste painting has been an effective method for depositing HTM thin films, but other methods (e.g., dip coating or spray deposition) might also be tested for fabricating thinner, stronger, defect-free thin films. To evaluate the performance of tubular HTMs, we will obtain a gas-tight seal by using the spring-loaded fixture developed in FY 2007. The hydrogen flux and permeability of HTM tubes will be measured in gases that simulate the atmosphere in "real-life" gasifiers; the tubes' flux and permeability will be monitored for periods of  $\approx 100$  h to evaluate their short-term chemical stability in syngas. The hydrogen flux and permeability of tubular membranes will be measured as a function of sweep and feed gas flow rates to determine more precisely the source of concentration polarization.

*Pd/Pd<sub>4</sub>S Phase Boundary.* Because HTMs will likely come into contact with H<sub>2</sub>S, which reacts with Pd-containing membranes to form Pd<sub>4</sub>S, we will continue to explore the effect of Pd<sub>4</sub>S-formation on the performance of HTMs. Based on our work during the past fiscal year and in FY 2006 [1], we know the position of the Pd/Pd<sub>4</sub>S phase boundary as a function of hydrogen concentration in the feed gas. With this information, we will be able to correlate hydrogen flux measurements with the phase boundary data. In particular, we will compare the hydrogen flux when Pd<sub>4</sub>S is stable to that when Pd is stable. To compare the behavior of Argonne's cermet membranes to metallic membranes, the flux will be measured for both cermet and metallic membranes on both sides of the phase boundary.

*High-Pressure Testing.* We will continue using Argonne's high-pressure reactor to study the performance of Argonne membranes and seals at high pressures, using  $\Delta p H_2^{1/2}$  values approaching  $\approx 3.5 \text{ atm}^{1/2}$ , where  $\Delta p H_2^{1/2}$  is defined in Eqn. (6). Because previous high-pressure measurements suggested that the flow rates of feed and sweep gases influence the flux under some conditions, we will investigate the effects of sweep and feed gas flow rates during our high-pressure flux measurements. The fixture for making high-pressure measurements will be modified to enable the testing of HTM tubes at high pressure.

*System Analyses.* The Aspen Plus<sup>®</sup> Simulation module will be used to evaluate the economics of an integrated gasification and combined cycle (IGCC) system for hydrogen production that employs HTMs for hydrogen purification. In our evaluation, we will compare the economics of an IGCC system operating at 900°C to one operating at 400°C. In addition to identifying novel equipment, estimating its cost, and considering challenges with interfacing the equipment with the overall system, we will explore opportunities to optimize the overall process. In particular, heat source temperature,

pressure and duty requirements, heat carrier medium, and conditions and purity of the process streams will be considered. While most of the plant will be based on well-understood equipment, we will need to develop user modules for the HTM units, because they represent a departure from commonly used equipment.

Evaluation of process issues and economics will continue as technical progress warrants. As directed through consultations with NETL's program managers, contacts will be made and discussions will be held with potential collaborators. We will work with NETL's in-house R&D team and their Systems Engineering Group to validate the process concept and conduct techno-economic evaluation of proton-conducting membrane technology for separating hydrogen in the power and petrochemical industries. We will provide technical input and engineering data to the NETL team to develop models for process viability and for thermal management studies.

## **VI. PUBLICATIONS AND PRESENTATIONS**

Transport Properties of  $\text{BaCe}_{0.95}\text{Y}_{0.05}\text{O}_{3-\alpha}$  Mixed Conductors for Hydrogen Separation, *Solid State Ionics*, 100, 45 (1997).

Development of Mixed-Conducting Oxides for Gas Separation, *Solid State Ionics*, 108, 363 (1998).

Development of Proton-Conducting Membranes, presented at the AIChE Annual Meeting, New Orleans, LA, March 9-13, 1998.

Mixed-Conducting Ceramic Membranes for Hydrogen Separation, presented at the 193<sup>rd</sup> Meeting of the Electrochemical Society, San Diego, CA, May 3-8, 1998.

Development of Mixed-Conducting Ceramic Membranes for Hydrogen Separation, *Ceramic Transactions*, 92, 1 (1998).

Development of Mixed-Conducting Dense Ceramic Membranes for Hydrogen Separation, *Proc. 5<sup>th</sup> Intl. Conf. Inorganic Membranes*, Nagoya, Japan, June 22-26, 1998, pp. 192-195.

Development of Proton-Conducting Membranes for Hydrogen Separation, presented at the Advanced Coal-based Power and Environmental Systems '98 Conference, Morgantown, WV, July 21-23, 1998.

The Effects of Dopants and A:B Site Nonstoichiometry on Properties of Perovskite-Type Proton Conductors, *J. Electrochem. Soc.*, 145, 1780 (1998).

Transport Properties of  $\text{SrCe}_{0.95}\text{Y}_{0.05}\text{O}_{3-\alpha}$  and its Application for Hydrogen Separation, *Solid State Ionics*, 110, 303 (1998).

High-Temperature Deformation of  $\text{BaCe}_{1-x}\text{Y}_x\text{O}_{3-y}$  ( $0.05 < x < 0.2$ ), *Solid State Ionics*, 117, 323 (1999).

Development of Mixed-Conducting Ceramics for Gas Separation Applications, *Mat. Res. Soc. Symp. Proc.*, 548, 545 (1999).

Performance Testing of Hydrogen Transport Membranes at Elevated Temperatures and Pressures, presented at Symposium on Hydrogen Production, Storage, and Utilization, New Orleans, Aug. 22-26, 1999; Am. Chem. Soc., Fuel Chem. Div., 44(4), 914 (1999).

Development of Mixed-Conducting Ceramic Membrane for Hydrogen Separation, presented at Sixteenth Annual International Pittsburgh Coal Conference, Pittsburgh, PA, Oct. 11-15, 1999.

Characterization of Ceramic Hydrogen Separation Membranes Containing Various Nickel Concentrations, presented at the Conference on Fossil Energy Materials -- Critical Supporting Technology R&D for Vision 21, Knoxville, TN, April 24-25, 2000.

Mixed Proton-Electron Conducting Cermet Membranes for Hydrogen Separation, presented at 102<sup>nd</sup> Annual Mtg. of the American Ceramic Society, St. Louis, MO, April 30-May 3, 2000.

Effect of Surface Modification on Hydrogen Permeation of Ni-BaCeO<sub>3</sub> Composites, presented at 102<sup>nd</sup> Annual Mtg. of the American Ceramic Society, St. Louis, MO, April 30-May 3, 2000.

Effect of Surface Modification on Hydrogen Permeation of Ni-BaY<sub>x</sub>Ce<sub>1-x</sub>O<sub>3.δ</sub> Composites, presented at 197<sup>th</sup> Meeting of the Electrochemical Society, Toronto, Ontario, Canada, May 14-19, 2000.

Evaluation and Modeling of a High-Temperature, High Pressure, Hydrogen Separation Membrane for Enhanced Hydrogen Production from the Water-Gas Shift Reaction, in "Advances in Hydrogen Energy," eds., C. E. G. Padro and F. Lau, Kluwer Academic/Plenum, New York, pp. 93-110 (2000).

Characterization of Ceramic Hydrogen Separation Membranes with Varying Nickel Concentrations, J. of Applied Surface Science, 167, 34 (2000).

The Crystal Structures and Phase Transitions in Y-doped BaCeO<sub>3</sub>: Their Dependence on Y-Concentration and Hydrogen Doping, Solid State Ionics, 138, 63 (2000).

Development of Dense Ceramic Membranes for Hydrogen Separation, Proc. 26<sup>th</sup> International Conference on Coal Utilization and Fuel Systems, Clearwater, FL, March 5-8, 2001, pp. 751-761.

Thin-Film Cermet Membrane Preparation for Hydrogen Separation, presented at 103<sup>rd</sup> Annual Meeting of the American Ceramic Society, Indianapolis, IN, April 22-25, 2001.

Surface Modifications of Hydrogen-Separation Membranes Based on the Mixed Conductor Ni-BCY, presented at 103<sup>rd</sup> Annual Meeting of the American Ceramic Society, Indianapolis, IN, April 22-25, 2001.

Development of Dense Ceramic Membranes for Hydrogen Separation, published in the Proceedings of the 6<sup>th</sup> Natural Gas Conversion Symposium, Girdwood, Alaska, June 17-22, 2001.

Development of Dense Ceramic Membranes for Hydrogen Separation, Proceedings of the 18<sup>th</sup> International Pittsburgh Coal Conference, Newcastle, Australia, Dec. 4-7, 2001, published by the Pittsburgh Coal Conference, University of Pittsburgh, Pittsburgh, PA.

Defect Chemistry Modeling of High-Temperature Proton-Conducting Cerates, Solid State Ionics, 149, 1 (2002).

Current Status of Dense Ceramic Membranes for Hydrogen Separation, Proceedings of the 27<sup>th</sup> International Technical Conference on Coal Utilization and Fuel Systems, Clearwater, FL, March 4-7, 2002, published by the Coal Technology Association, Gaithersburg, MD.

Dense Ceramic Membranes for Hydrogen Separation, presented at the 16<sup>th</sup> Annual Conference on Fossil Energy Materials, Baltimore, MD, April 22-24, 2002.

Hydrogen Production by High-Temperature Water Splitting Using Mixed Oxygen Ion-Electron Conducting Membranes, Proc. 201<sup>st</sup> Electrochem. Soc. Mtg., Philadelphia, PA, May 12-17, 2002.

Effect of Pd Coating on Hydrogen Permeation of Ni-Barium Cerate Mixed Conductor, Electrochemical and Solid-State Letters, 5(3), J5 (2002).

Electrical Properties of p-type Electronic Defects in the Protonic Conductor  $\text{SrCe}_{0.95}\text{Eu}_{0.05}\text{O}_{3-\delta}$ , J. Electrochem. Soc., 150(6), A790 (2003).

Interfacial Resistances of Ni-BCY Mixed-Conducting Membranes for Hydrogen Separation, Solid State Ionics, 159, 121 (2003).

Defect Structure and n-Type Electrical Properties of  $\text{SrCe}_{0.95}\text{Eu}_{0.05}\text{O}_{3-\delta}$ , J. Electrochem. Soc., 150, A1484 (2003).

Hydrogen Production by Water Splitting Using Mixed Conducting Membranes, Proc. National Hydrogen Assoc. 14<sup>th</sup> Annual U.S. Hydrogen Meeting, Washington, DC, March 4-6, 2003.

Current Status of Mixed-Conducting Ceramic Membranes for Gas Separation Applications, presented at the Univ. of Houston, March 14, 2003.

Dense Cermet Membranes for Hydrogen Separation, presented at the 225<sup>th</sup> Amer. Chem. Soc. Natl. Mtg., Fuel Chemistry Div., New Orleans, March 23-27, 2003.

Hydrogen Production by Water Dissociation Using Mixed-Conducting Membranes, presented at 225<sup>th</sup> Amer. Chem. Soc. Natl. Mtg., Fuel Chemistry Div., New Orleans, March 23-27, 2003.

Current Status of Mixed-Conducting Ceramic Membranes for Gas Separation Applications, presented at the University of Illinois, Urbana-Champaign, April 24, 2003.

Hydrogen Production by Water Dissociation Using Oxygen-Permeable Cermet Membranes, presented at 105<sup>th</sup> Ann. Mtg. of Amer. Ceramic Soc., Nashville, April 27-30, 2003.

Preparation and Characterization of New Mixed Conducting Oxides  $\text{Ba}(\text{Zr}_{0.8-x}\text{Pr}_x\text{Y}_{0.2})\text{O}_{2.9}$ , presented at 105<sup>th</sup> Ann. Mtg. of Amer. Ceramic Soc., Nashville, April 27-30, 2003.

Metal/Ceramic Composites with High Hydrogen Permeability, U.S. Patent #6,569,226, May 27, 2003.



Current Status of Dense Cermet Membranes for Hydrogen Separation, presented at the 20<sup>th</sup> Annual Intl. Pittsburgh Coal Conf., Pittsburgh, Sept. 15-19, 2003; in Conf. Proc., S46, 187.PDF, 2003.

Current Status of Ceramic Membranes for Hydrogen Production and Separation Applications, presented at the U. of Alaska-Fairbanks, Sept. 24, 2003.

Hydrogen Production by Water Dissociation Using Mixed Conducting Membranes, presented at Second Information Exchange Meeting on Nuclear Production of Hydrogen, Argonne Natl. Lab., Oct. 2-3, 2003.

A Method to Remove Ammonia using a Proton-Conducting Membrane, U.S. Patent #6,630,116, Oct. 7, 2003.

Numerical Modeling of Hydrogen Permeation in Chemical Potential Gradients, Solid State Ionics, 164, 107 (2003).

Development of Dense Cermet Membranes for Hydrogen Separation, presented at the 204<sup>th</sup> Mtg. of the Electrochemical Soc., Orlando, Oct. 12-17, 2003.

Hydrogen Permeation of Cermet  $\text{Ba}(\text{Ce}_{0.6}\text{Zr}_{0.2})\text{Y}_{0.2}\text{O}_3/\text{Ni}$  Membranes, presented at the 204<sup>th</sup> Mtg. of the Electrochemical Soc., Orlando, Oct. 12-17, 2003.

Hydrogen Permeability of  $\text{SrCe}_{1-x}\text{M}_x\text{O}_{3-d}$  ( $x = 0.05$ ,  $\text{M} = \text{Eu}, \text{Sm}$ ), Solid State Ionics, 167, 99 (2004).

Use of Mixed Conducting Membranes to Produce Hydrogen by Water Dissociation, Intl. J. Hydrogen Energy, 29, 291-296 (2004).

Hydrogen Production by Water Dissociation using Mixed-Conducting Ceramic Membranes, Proc. of National Hydrogen Assoc. 15<sup>th</sup> Annual U.S. Hydrogen Energy Conf., Los Angeles, CA, April 27-30, 2004.

Mixed-Conducting Dense Ceramic Membranes for Hydrogen Production and Separation from Methane, presented at 15<sup>th</sup> World Hydrogen Energy Conf., Yokohama, Japan, June 27-July 2, 2004.

Hydrogen Production from Water Using Mixed-Conducting Ceramic Membranes, presented at 15<sup>th</sup> World Hydrogen Energy Conf., Yokohama, Japan, June 27-July 2, 2004.

Development of Dense Ceramic Membranes for Hydrogen Production and Separation, Proc. of 8<sup>th</sup> Intl. Conf. on Inorganic Membranes, eds., F. T. Akin and Y. S. Lin, Adams Press, Chicago, IL (2004), pp. 163-166.

Development of Dense Cermet Membranes for Hydrogen Separation, presented at 21<sup>st</sup> Annual Intl. Pittsburgh Coal Conf., Osaka, Japan, Sept. 13-17, 2004.

Hydrogen Permeation of Cermet  $[\text{Ni}-\text{Ba}(\text{Ce}_{0.6}\text{Zr}_{0.2})\text{Y}_{0.2}\text{O}_{3-\delta}]$  Membranes, presented at the 206<sup>th</sup> Mtg. of the Electrochemical Soc., Honolulu, Oct. 3-8, 2004.

Development of Dense Ceramic Membranes for Hydrogen Production and Separation, presented at American Soc. for Materials--Annual Materials Solution Conf., Columbus, OH, Oct. 18-21, 2004.

Electrical and Hydrogen Transport Properties of  $\text{SrCe}_{0.8}\text{Yb}_{0.2}\text{O}_{3-\delta}$ /Ni Cermet Membranes, presented at Fall Meeting of Materials Research Society, Boston, Nov. 29-Dec. 3, 2004.

Preparation and Hydrogen Pumping Characteristics of  $\text{BaCe}_{0.8}\text{Y}_{0.2}\text{O}_{3-\delta}$  Thin Film, presented at Fall Meeting of Materials Research Society, Boston, Nov. 29-Dec. 3, 2004.

Hydrogen Permeability and Microstructure Effect of Mixed Protonic-Electronic Conducting Eu-Doped Strontium Cerate, J. Mater. Sci., 40, 4061-4066 (2005).

Defect Structure and Transport Properties of  $\text{Ni-SrCeO}_{3-\delta}$  Cermet for Hydrogen Separation Membrane, J. Electrochem. Soc. 152(11), J125 (2005).

Dense Cermet Membranes for Hydrogen Separation, presented at American Institute of Chemical Engineers (AIChE) Spring National Meeting, Atlanta, GA, April 10-14, 2005.

Hydrogen Separation Using Dense Cermet Membranes, presented at 30<sup>th</sup> Intl. Tech. Conf. on Coal Utilization and Fuel Systems, Clearwater, FL, April 17-21, 2005.

Electrical and Hydrogen Transport Properties of  $\text{SrCe}_{0.8}\text{Yb}_{0.2}\text{O}_{3-\delta}$ /Ni Cermet Membranes, Mat. Res. Soc. Symp. Proc., 835, K3.2 (2005).

Preparation and Hydrogen Pumping Characteristics of  $\text{BaCe}_{0.8}\text{Y}_{0.2}\text{O}_{3-\delta}$  Thin Film, Mat. Res. Soc. Symp. Proc., 835, K1.5 (2005).

Structure, Proton Incorporation and Transport Properties of Ceramic Proton Conductor  $\text{Ba}(\text{Ce}_{0.7}\text{Zr}_{0.2}\text{Yb}_{0.1})\text{O}_{3-\delta}$ , Mat. Res. Soc. Symp. Proc., 835, K1.4 (2005).

Development of Dense Ceramic Membranes for Hydrogen Separation, presented at 2005 DOE Annual Hydrogen Program Review, Washington, DC, May 23-25, 2005.

Membranes: The Good, The Bad, and The Ugly, presented to Hydrogen & Fuel Cell Tech. Prog. Office, DOE, Wash., DC, June 8, 2005.

Thin Film Preparation and Hydrogen Pumping Characteristics of  $\text{BaCe}_{0.8}\text{Y}_{0.2}\text{O}_{3-\delta}$ , Solid State Ionics, 176, 1479-1484 (2005).

Hydrogen Production by Water Splitting Using Dense Thin-Film Cermet Membranes, presented at Fall Meeting Materials Research Society, Boston, Nov. 28-Dec. 2, 2005.

Hydrogen Permeation and Chemical Stability of Cermet  $[\text{Ni-Ba}(\text{Zr}_{0.8-x}\text{Ce}_x\text{Y}_{0.2})\text{O}_3]$  Membranes, Electrochem. & Solid State Lett., 8(12), J35-J37 (2005).

Electrochemical Hydrogen Pumping Characteristics of  $\text{BaCe}_{0.8}\text{Y}_{0.2}\text{O}_{3-\delta}$  Thin Film, presented at Electrochem. Soc. 2005 Fall Mtg., Los Angeles, Oct. 16-21, 2005.

Defect Structure and Transport Properties of  $\text{Ni-SrCeO}_{3-\delta}$  Cermet for Hydrogen Separation Membrane, J. Electrochem. Soc., 152 (11), J125, 2005.

Review: Stress-Induced Diffusion and Cation Defect Chemistry Studies of Perovskites, invited paper published in "Defects & Diffusion in Ceramics – An Annual Retrospective VII; Defect & Diffusion Forum," Scitech Publication, London, UK (Oct. 2005), pp. 43-63.

Hydrogen Production by Water Dissociation Using Mixed Oxygen Ion-Electron Conducting Membranes, presented at Electrochem. Soc. 2005 Fall Mtg., Los Angeles, Oct. 16-21, 2005.

Hydrogen Permeation of Ceramic/Metal Composite Thin Films, presented at Electrochem. Soc. 2005 Fall Mtg., Los Angeles, Oct. 16-21, 2005.

Development of Dense Cermet Membranes for Hydrogen Separation, invited presentation at World Hydrogen Technologies Convention, Singapore, Oct. 3-6, 2005.

Mixed-Conducting Dense Ceramic Membranes for Air Separation and Natural Gas Conversion, J. Solid State Electrochem., 10, 617-624 (2006).

Hydrogen Separation by Dense Cermet Membranes, Fuel, 85(2), 150-155 (2006).

Hydrogen Production by Water Dissociation Using Mixed-Conducting Dense Ceramic Membranes, invited presentation at Amer. Chem. Soc. 231<sup>st</sup> Natl. Mtg., Atlanta, March 26-30, 2006.

Development of Dense Membranes for Hydrogen Production and Separation, Invited Talk at the 2<sup>nd</sup> Energy Center Hydrogen Initiative Symposium, Purdue University, West Lafayette, IN, April 12-13, 2007.

Development of Dense Cermet Membranes for Hydrogen Separation, presented at AIChE Spring Mtg., Orlando, FL, April 23-27, 2006.

Hydrogen Production from Methane Using Dense Oxygen and Hydrogen Transport Membranes, presented at 209th Electrochemical Soc. Mtg., Denver, May 7-12, 2006.

Development of Dense Hydrogen Transport Membranes, presented at the 31<sup>st</sup> International Technical Conference on Coal Utilization and Fuel Systems, Clearwater, FL, May 21-25, 2006.

Annealing Effect of Cermet Membranes on Hydrogen Permeability, Chem. Lett., 35(12), 1378-1379 (2006).

Mixed-conducting Membranes for Hydrogen Production and Separation, Invited presentation at 2006 MRS Fall Meeting, Boston, MA, Nov. 27 – Dec. 1, 2006.

Dense Cermet Membranes for Hydrogen Separation from Mixed Gas Streams, presented at 23<sup>rd</sup> Annual Intl. Pittsburgh Coal Conf., Pittsburgh, PA, Sept. 25-28, 2006.

Effect of Zr-Doping on the Chemical Stability and Hydrogen Permeation of the Ni-BaCe<sub>0.8</sub>Y<sub>0.2</sub>O<sub>3-δ</sub> Mixed Protonic-Electronic Conductor, Chemistry of Materials, 18(19), 4647 (2006).

Composite Ni-Ba(Zr<sub>0.1</sub>Ce<sub>0.7</sub>Y<sub>0.2</sub>)O<sub>3</sub> Membrane for Hydrogen Separation, J. Power Sources, 159(2), 1291 (2006).

Dense Membranes for Hydrogen Separation and Purification, to be published in "Materials for the Hydrogen Economy," CRC Press LLC, Boca Raton, FL, 2007.

Stability of Dense Cermet Membranes for Hydrogen Separation, presented at 211<sup>th</sup> Meeting of Electrochemical Society, Chicago, IL, May 6-10, 2007.

Development of Dense Membranes for Hydrogen Production from Coal, Invited Talk at 234<sup>th</sup> American Chemical Society National Meeting, Boston, MA, Aug. 19-23, 2007.

Chemical Stability of Hydrogen Transport Membranes, presented at the 24<sup>th</sup> Annual International Pittsburgh Coal Conference, Johannesburg, South Africa, Sept. 10-14, 2007.

## REFERENCES

1. U. Balachandran, Argonne National Laboratory Hydrogen Separation Membranes-- Annual Report for FY 2006.
2. J. R. Taylor, *Met. Trans.*, **16B**, 143-148 (1985).
3. O. Knacke, O. Kubaschewski, and K. Hesselmann, *Thermochemical Properties of Inorganic Substances*, Vol. I, 2nd Ed., Springer-Verlag, Berlin (1991).
4. U. Balachandran, Argonne National Laboratory Hydrogen Separation Membranes-- Quarterly Report for October-December 2006.
5. T. Matsui, M. Harada, M. Toba, and Y. Yoshimura, *Appl. Catal. A*, **293**, 137-144 (2005).
6. H. Yasuda and Y. Yoshimura, *Catal. Lett.*, **46**, 43-48 (1997).
7. U. Balachandran, Argonne National Laboratory Hydrogen Separation Membranes-- Annual Report for FY 2005.
8. U. Balachandran, Argonne National Laboratory Hydrogen Separation Membranes-- Quarterly Report for January-March 2007.
9. S. A. Koffler, J. B. Hudson, and G. S. Ansell, *Trans. Met. Soc. AIME*, **245**, 1735 (1969).



## **Energy Systems Division**

Argonne National Laboratory  
9700 South Cass Avenue, Bldg. 212  
Argonne, IL 60439-4838

[www.anl.gov](http://www.anl.gov)



UChicago ►  
Argonne<sub>LLC</sub>

A U.S. Department of Energy laboratory  
managed by UChicago Argonne, LLC